

Mario CASTILLO NEVOT



Escuela de  
Ingeniería y Arquitectura  
Universidad Zaragoza

# ANALYSIS OF A HYBRID PROPULSION SYSTEM FOR A ULTRA LIGHT AIRCRAFT

*Bachelor thesis submitted as fulfillment of the requirements for  
the degree of Civil Mechanical Engineering*

University of Liege  
Faculty of Applied Sciences  
Academic Year 2023-2024

## Abstract

This project aims to test the combination of existing equipment to obtain efficient hybrid-electric propulsion for a microlight aircraft which fits the ULM description and has a MTOW of 530 kg. Some of the additional objectives would be to dimension a battery, get data for the possible emissions of the system, study efficiencies of various components and an estimation of the costs. The main tool employed for the achievement of these objective consist of developing a working simulation via the software AMESim. This software allows for the user to implement all the data available in wide range of degrees of precision and simulate a flight mission of a hybrid series powertrain plane, to see how each of the components react during the duration of said flight. We are able to study the behaviour of the ICE, the generator, the battery, the electric motor and more. The software offers graphs and predictions on a huge number of variables thanks to its many submodels from which conclusions will be drawn to better understand the key points of this design. With all the collected data, completion of the proposed flight mission was achieved when including all the selected components. Estimations on the operational costs and exhaust gases came as a result as well. The most susceptible to improvement parts of the design were identified and recommendations were made for future research.

## Acknowledgments

Firstly, I would like to thanks the Mechanical and Aerospace Department of the University of Liege for allowing me to participate in such an amazing project which has taught me a lot.

Also, I must thank my supervisor Professor Loïc Salles for guiding me during the process and helping me understand many concepts that I wasn't familiar with as well as understanding all the difficulties and challenges that I have had to face. I must thank our promoter Gaël Minne for making this project possible and always being open to help me whenever I had doubts about the details of the plane or topics related to it. I would like to thank Professor Emin Oguz Inci from the KU Leuven to help me solve my problems with the software AMESim.

Also, I would like to thank the jury for accepting my decision to present in June and evaluating my work.

Finally, I am extremely thankful to my family and friends both from Spain and Belgium for supporting me through the process and believing in me every day. Especially, I have to thank to my peers in similar projects, Charles and Colette, who have always answered my questions.

# Contents

<b>1</b>	<b>Introduction</b>	<b>4</b>
1.1	Background	4
1.2	Motivation	5
1.3	Objectives	6
1.4	Tools	8
<b>2</b>	<b>State of the art</b>	<b>9</b>
2.1	Hybridization of planes	9
2.1.1	Types of configurations	11
2.1.2	Description of simulation	14
2.1.3	Existing models	29
2.2	Design of airplane's frame	31
2.2.1	Ultra light aircraft definition - Weight of the plane	32
2.2.2	Geometry	33
2.3	Internal combustion engine	34
2.3.1	Rotax: engines and applications	35
2.3.2	Rotax 912 UL	37
2.4	Generator	40
2.4.1	Safran: leaders in electrical propulsion	40
2.4.2	GENeUS	41
2.5	Electrical motors	42
2.5.1	ENGINus 100	42
2.6	Battery	43
2.6.1	Safran: power storage and the GENeUSPACK	44
2.7	Propeller	45
2.8	TurboGenerator	47
<b>3</b>	<b>Simulation in AMESim</b>	<b>50</b>
3.1	Characterising components and assumptions	50
3.1.1	Mission Plan	50
3.1.2	Atmospheric conditions	51
3.1.3	Control section	52
3.1.4	Engine Characterisation	53
3.1.5	Generator and Motor Characterisation	56
3.1.6	Battery	57
3.1.7	Aerodynamics and weight	60
<b>4</b>	<b>Results and discussion</b>	<b>63</b>
4.1	Plots and graphs	63
4.2	Plots and graphs - TurboGenerator	70

4.3 Interpretation of data and findings . . . . .	72
<b>5 Conclusion and future works</b>	<b>74</b>

# Chapter 1

## Introduction

### 1.1 Background

A new trend is begging to show in most technological fields which rely on the usage of traditional combustion engines or any kind of combustion reaction since there is numerous scientific research that demonstrates how harmful it is to both the environment and everybody's long term health. This new trend is triggered by initiatives that have been stated globally in order to fight the negatives effects of the pollution that contaminates our air, our soil and our water.

One crucial initiative such as the formerly mentioned would be the Agenda 2030. This plan was agreed upon by the countries' leaders members of the United Nations Organization on September 2015, in the UN headquarters of New York. The Agenda 2030 presents a total of 17 objectives or, as they are called Sustainable Development Goals 1.1 and marked a significant global commitment to addressing pressing social, economic, and environmental challenges over the next 15 years. The goals are as follow, according to [30]:

- 1. No Poverty
- 2. Zero Hunger
- 3. Good Health and Well-being
- 4. Quality Education
- 5. Gender Equality
- 6. Clean Water and Sanitation
- 7. Affordable and Clean Energy
- 8. Decent Work and Economic Growth
- 9. Industry, Innovation, and Infrastructure
- 10. Reduced Inequality
- 11. Sustainable Cities and Communities
- 12. Responsible Consumption and Production
- 13. Climate Action

- 14. Life Below Water
- 15. Life on Land
- 16. Peace, Justice, and Strong Institutions
- 17. Partnerships for the Goals



Figure 1.1 - *UN Initiatives for the future*

These objectives were preceded by another set of similar aims called the Millennium Development Goals (MDGs). Thus we can clearly define a path of global collaboration that not only will last for another period of fifteen years but also Will last in our future and in that of other generations.

Finally, if we are aware that this is what our prospects look like, why shall we not take part in it?

## 1.2 Motivation

This project's primarily aims is to contribute to the fields of electrification and hybridization as well as to give a little push to the idea that these concepts may also be applied in fields not considered in the first place such as aviation and aircraft propulsion. The pursuit of more sustainable and Eco-friendly way to transport goods and people thought the skies is a very ambitious and difficult goal at the same time although breakthroughs are bound to be made due to all the interests this topic can muster.

Relating to the aforementioned objectives, this project seeks to contribute in its own capacity and offer some guidance on some of the SDGs. In fact, the project is directly related to some of those initiatives which will be explain shortly.

- (a) Firstly, goal number 7 "Affordable and Clean Energy" is clearly related to the objectives of my work since the main point of employing hybridization and electrification in our devices is to eliminate the need for fossil fuels and other more pollutant sources

of energy, and to exchange them for the cleaner alternative that is electricity which will not only lead to a healthier environment but more independent countries as well.

- (b) Secondly, goal number 9 "Industry, Innovation and Infrastructure" is heavily influenced by factors such as the advancements of hybrid technologies, batteries and power distribution systems. There are entire networks of industries and markets based on every single component of my research and larger and larger amounts of capital both monetary and human are invested each year.
- (c) Thirdly, goal number 13 "Climate Action" shares values with the purpose of the project because hybridization is one of the most immediate tools to solve the climate crisis. Hybrid engines present a higher efficiency than regular combustion engines thus diminishing the amount of emissions. Also they allow the possibility for multiple ways of generating electrical power which implies that, as the generating methods shift towards clean/renewable energy sources, the environmental benefits of hybridization will increase accordingly.

There are other SDGs that could be linked to this project for example number 3 or number 12 which are "Good health and Well-being" and "Responsible Consumption and Production" respectively. However, since the connection is not direct and other factors should be taken into account to evaluate the relevance of innovation of hybrid technology in health and production/consumption practices, they will not be included as motivation factors.

### 1.3 Objectives

In this project, our objectives are manifold, all centered around the validation and integration of hybridization technologies into novel applications where their utilization has thus far been limited. Furthermore, we seek to pave the way for their widespread adoption in sectors where they have yet to be fully explored or exploited.

Some prime examples of the unusual union of the electrification and aviation fields have succeeded in creating an efficient working model. Such creations would be the eFlyer 2 from Bye Aerospace 1.2, the E-Fan 1.3 and the E-Fan X 1.4 from Airbus.



Figure 1.2 - *eFlyer 2 from Bye Aerospace*



Figure 1.3 - *E-Fan from Airbus*



Figure 1.4 - *E-Fan X from Airbus*

Even though the aims of this project are numerous, some of its most important ones can be summarised :

- Construct an accurate simulation of the entire propulsion system taking into account all the relevant components of the plane and be able to alter the parameters, measurements and values of each components so as to study its impact on the flight and its consequences.
- Track and plot results that show the evolution of crucial aspects in the aviation field. Some of these variable could be:
  - Fuel consumption
  - Battery percentage and temperature
  - Mass of the aircraft
  - Noise produced
  - Power output
- Find the best combination of combustion and electrical power with the intention of maximising range, autonomy and power output but minimizing the noise, emission and costs.

## 1.4 Tools

Numerous tools exist for modeling complex systems, yet few possess the requisite flexibility to integrate diverse concepts originated from fields like avionic, electricity, thermodynamics, heat transfer, aerodynamics, mechanics and physics. The predominant software used must facilitate the amalgamation of various components and variables, while concurrently ensuring monitoring and management of said quantities.

Considering these criteria, my academic advisor came to the conclusion that a highly specialized software solution was in order. After some deliberation, the answer to this question materialized in a product from a reputable entity: Siemens

Simcenter AMESim is the designated software that will be employed to model the simulation for this project. This program was selected over other options that present similar capabilities and are much more popular in academic works like Matlab/Simulink or Modelica for several reasons which will be outlined below:

- (a) AMESim offers the opportunity of working with multi domain simulations by letting us construct dynamic schematic physical systems that imitate the real ones with high accuracy. These systems crafted from the combination of many components belonging to advanced component libraries, specialized solvers, and dedicated analysis tools that are well-suited to the requirements of most projects
- (b) While Matlab/Simulink and Modelica are well established in the academic environment, the usage of AMESim is an industry standard tool extensively used by many engineering and industrial companies, therefore ensuring compatibility and connection with the actual working world
- (c) At a more academical level, one of the most notable merits of AMESim lies in the wealth of tutorials and comprehensives courses. This resources explain step by step the software's intricacies and provide the user with enough expertise to efficiently maneuver across the system and accomplish simple tasks. Besides, in case of specific inquiries pertaining to a particular component, AMESim posses a help menu which contains information about not only each component but also any preconstructed simulations.
- (d) This software is designed to integrate projects made by using other tools and thus reinforcing the possibility for cooperation between enterprises, streamlining the modeling process and improving efficiency overall.
- (e) Another notable advantage demonstrated by AMESim is its superior performance and scalability compared to other software according to [13], particularly concerning large-scale simulations. This is facilitated by the Performance Analyzer tool, which enables a detailed examination of computational time contributions and discontinuities

# Chapter 2

## State of the art

### 2.1 Hybridization of planes

Hybridization is defined as the technique of integrating different sources of energy into one single system of propulsion for a vehicle. In fact, hybrid vehicles are almost as old as the automobile itself according to [14], since the first HEVs date as far as the Paris Salon of 1899 and they were actually built by the Pieper establishments of Liège, Belgium and by the Vedovelli and Priestly Electric Carriage Company. A couple of years later, in 1901, Ferdinand Porche creates the Lohner-Porsche Mixte 2.1, another model which will mark the birth of a new race of automobiles. From that point forward, numerous car companies have came into the industry and competed to devise their own hybrid electric vehicles with some notable breakthroughs like the introduction of the Toyota Prius, the first mass produce hybrid vehicle, in 1997. In 2012, Tesla released the Model S, a luxury sedan with long driving capabilities. A great number of advancements in elements like batteries, electric motors and overall design of vehicles have been made in the latest years.

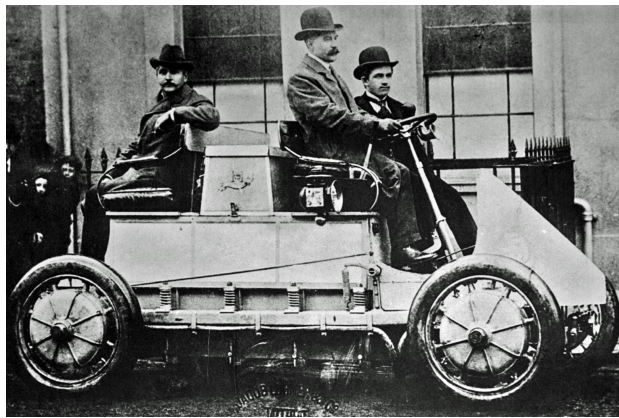


Figure 2.1 - *Lohner Porsche Mixte from 1901*

Hybridization is predominantly observed within the automotive sector, whereas its integration within the aerospace domain remains limited. The implementation of hybrid technologies is notably more feasible within automotive designs than within the complex structural and operational requirements of an aircraft. Additionally, the automotive industry often benefits from significant revenue streams leading to greater enthusiasm for technological innovation. In contrast, the motivations driving hybridization efforts within aviation are generally more modest.

There are a great amount of challenges which make difficult the implementation of hybrid technologies in the field of avionics.

The first and most crucial is the total weight of the aircraft. Aircraft are extremely sensitive to weight changes since they depend on lift, a force generated thanks to the airfoil which propels them upwards while the weight does the opposite. For example, in order to maintain an airplane during the cruise phase of its journey, the following condition must be accomplished:

$$L_{\text{required}} = W$$

where:  $L_{\text{required}}$  is the required lift, and  $W$  is the total weight of the plane.

The equation for weight is given by:

$$W = m * g \quad (2.1)$$

where  $W$  is the weight,  $m$  is the mass, and  $g$  is the acceleration due to gravity.

According to 2.1, the weight is directly proportional to the mass of the aircraft and thus the mass of each of its components. Therefore, by adding hybrid components, such as batteries and electric motors, it increases the overall weight of the aircraft and then additional weight must be carefully balanced against the desired benefits of hybridization. In many cases, this balance does not result in viable or economically feasible solutions and the idea of hybridising a certain design is scrapped.

Yet another constrain that must be taken into account is the way the weight is distributed because the location of the center of gravity is critical for maintaining stability and maneuverability during flight. Achieving a good placement of the center of gravity while integrating hybrid components might prove too challenging. This is related to the amount of space available in the air frame, since each component occupies and compromises a certain amount of volume which could have been destined to house the payload or other critical equipment. Additional space provided by modifications on the external shape or surface of the plane must be carefully design in order to minimize drag and maintain optimal aerodynamic performance.

Furthermore, the topic of security and regulation must be addressed. At first, a hybrid design for a plane seems a more secure option since, in the case of one of the two power sources failing, the plane could rely on the other one to safely complete its flight mission or perform an emergency landing in a more secure area. Nevertheless, by adding more components, the aircraft's design gets more and more complex, allowing for even more ways for it to malfunction or fail. This paradox can be solved by setting standards such as test and trials, and establishing new regulations regarding safety and airworthiness for any design containing hybrid technologies. Although this approach may seem obvious and necessary, it ultimately goes against innovation and the proliferation of hybrid technology by establishing technical obstacles for engineers and economic barriers for investors.

Finally, an overarching challenge compounding the already mentioned barriers is the lack of advanced enough technologies enabling hybrid models to effectively rival conventional jet aircraft. The range and endurance achieved by current battery technology or hybrid propulsion systems notably lags behind their combustion-based counterparts. Also, the current landscape neither renders mass production of such technology feasible nor there is enough infrastructure such as charging stations or alternative fuel cells to support its widespread adoption.

## 2.1.1 Types of configurations

The architecture of a hybrid vehicle is loosely defined as the connection between the components that define the energy flow routes and control ports. At first, the classification was very simple, there were series and parallel designs, although in the early 2000's, some new models were developed and couldn't be classified in one of these two groups. Hence a new classifications was devised, according to [14]:

- (a) Series Hybrid
- (b) Parallel Hybrid
- (c) Series-Parallel hybrid
- (d) Complex hybrid

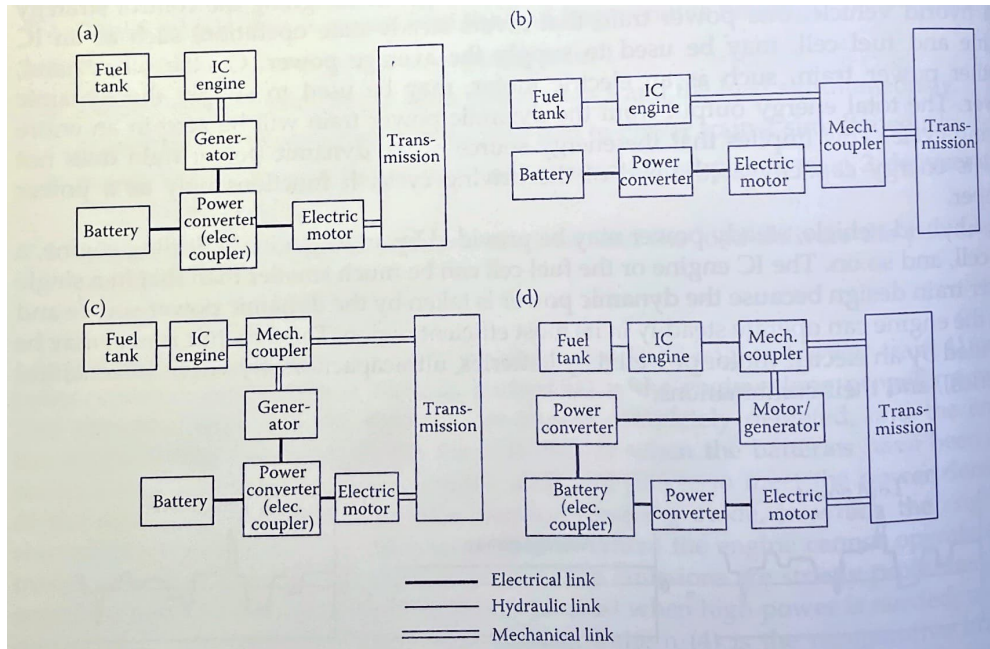


Figure 2.2 - *Types of architectures for HEV*

There is yet another way to differentiate the architectures of an HEV that is based on the power coupling or decoupling system. This gives us a new manner of classification:

- Electrical Coupling Drivetrain
- Mechanical Coupling Drivetrain
- Mechanical-Electrical Coupling Drivetrain

The two most common configurations and the ones that these project will focus on are the ones following:

- Series Hybrid Electric Drivetrains (Electrical Coupling):

This type of drivetrain is the one in which two electric power sources feed a single electrical power plant (electric motor) which is responsible for the propulsion of the vehicle. It consists of a unidirectional energy source which is a fuel tank and an unidirectional energy converter which is an ICE that is coupled to an electric generator. The output of the electric generator is connected to a power DC bus through a rectifier. Then, the bidirectional energy source is a battery pack connected to the same power DC bus by a controllable, bidirectional power electronic converter (DC/DC converter). Finally, the electrical coupler supplies the motor controller and the electrical motor with enough power to move the vehicle. This configuration allows for many different operation modes:

- Pure electric traction mode
- Pure engine traction mode
- Hybrid traction mode
- Engine traction with battery charging mode
- Regenerative braking mode
- Battery charging mode
- Hybrid battery charging mode

This configuration offers several advantages such as the possibility of operating the engine within its maximum efficiency region because it isn't mechanically connected to the wheels, as we can see in 2.3, and an overall greatly simplified drivetrain due to the similar torque-speed profile of electric motors and traction.

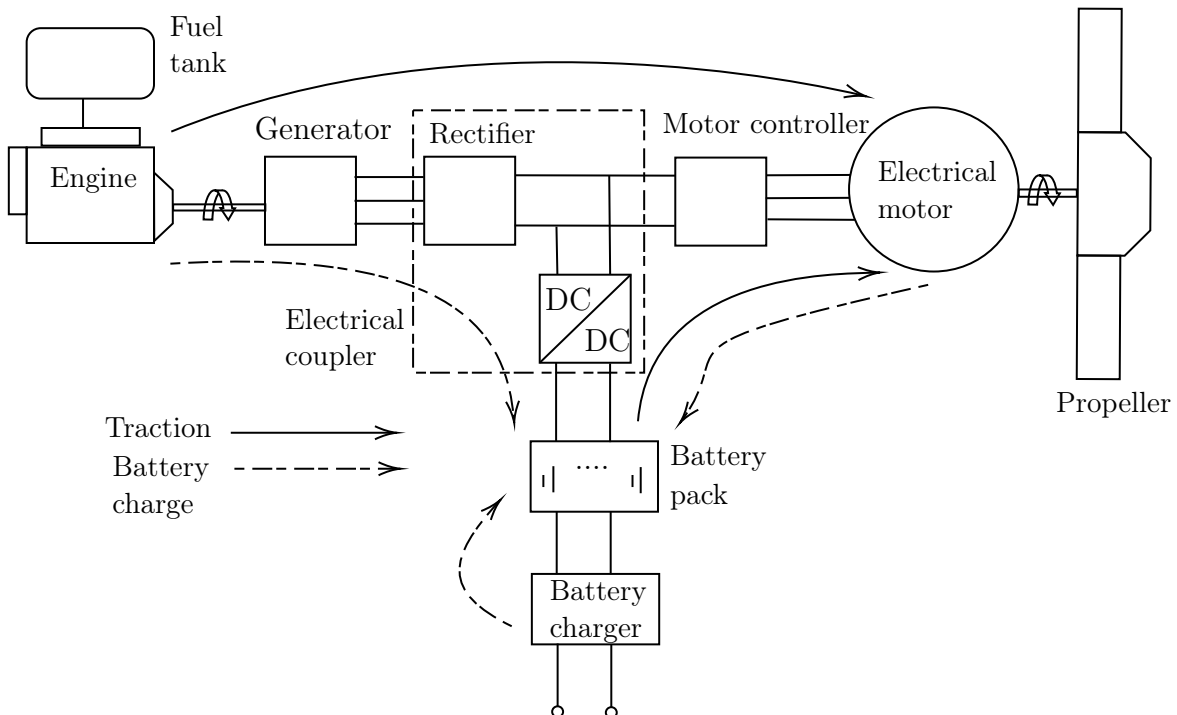


Figure 2.3 - Diagram of a Series Hybrid Electrical Coupling Drivetrain

The main disadvantage of this system would be the losses produced during the two changes of energy form occurred in the generator (mechanical to electrical) and the electrical motor (electrical to mechanical)

- Parallel Hybrid Electric Drivetrains (Mechanical Coupling)

This sort of hybrid drivetrain is the one in which the engine supplies its mechanical power directly to the propeller although it is assisted by the an electric motor that is mechanically coupled to the driveline. Therefore, the distinguishing feature of this design is that two mechanical powers from the engine and the electric motor converge my a mechanical coupler. Generally, mechanical coupling consists of torque coupling, speed coupling or both.

All the possible operating modes mentioned in the series hybrid drivetrain are still effective.

The major advantages of the parallel hybrid, which can be observed in the diagram 2.4, are that both the IC engine and the electrical motor supply torque to the propeller thus minimizing the losses energy, as no energy form conversion occurs, and no additional generator is needed to power the electric motor.

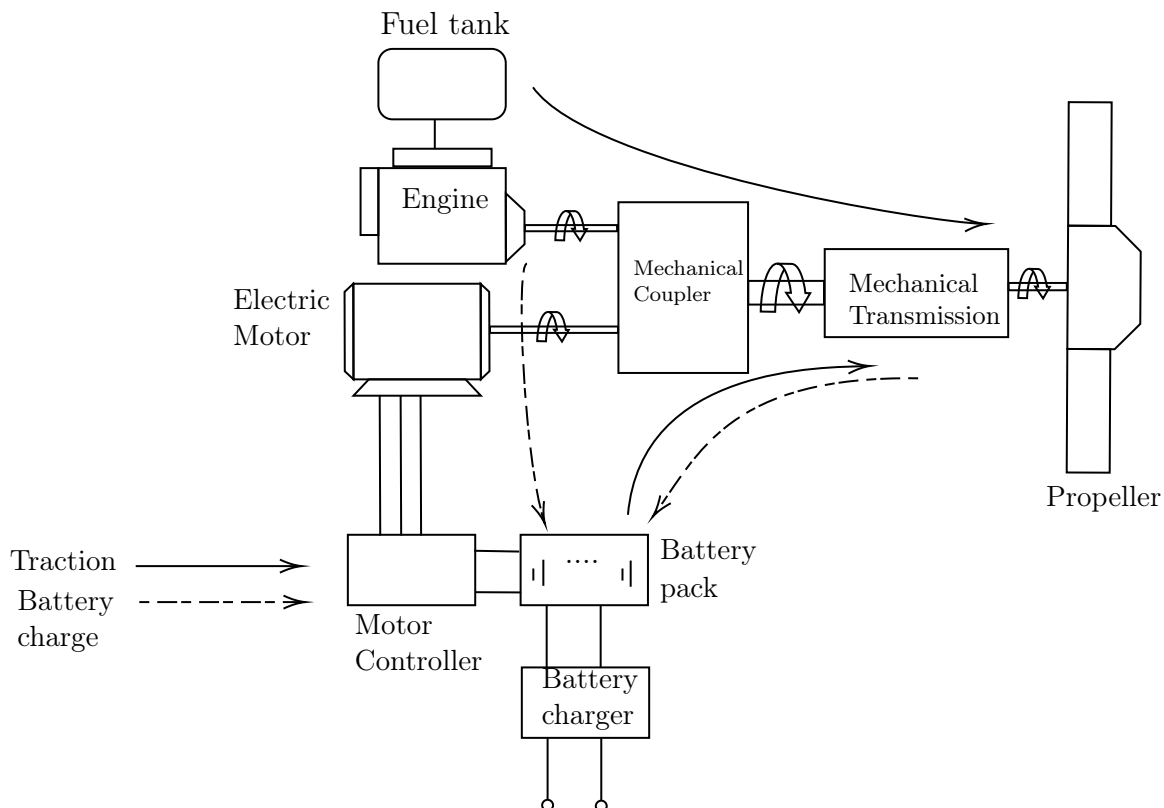


Figure 2.4 - Diagram of a Parallel Hybrid Mechanical Coupling Drivetrain

While such configurations present numerous advantages, they also exhibit certain weaknesses. Foremost among these is the necessity to incorporate a mechanical coupling between the engine and the propeller, since the engine operating points cannot

be fixed in a narrow speed or torque region due to the different sources of motion (ICE + E-motor). The inclusion of a mechanical coupling results in a control system that is inherently complex in both structure and control, thus rendering it not optimal for aviation applications where simplicity, weight, and volume are of paramount importance.

Once evaluated both principal configurations and after much delivering, the conclusion and outcome was that the best alternative would be to design a system portraying the Series Hybrid Electric Drivetrain. This would not only offer a simpler control system but, if the requirements are well defined and can be successfully met, the dimensioning of certain components would make the aircraft lighter and more maneuverable than another counterpart featuring a parallel design.

### 2.1.2 Description of simulation

Thanks to the use of Simcenter AMESim, access to multiple preconstructed simulations was possible. One of them accurately represent the propulsion system of a hybrid aircraft aircraft which could easily be modified to best fit the real design. From all the propulsion systems demos, the Serial-hybrid propulsion model was chosen.

As the manual [33] explains, this demo showcases the presizing of a hybrid electric propulsion unit used to propel a general aviation aircraft. This simulation can be used to, given a flight path designed by the user, later draft other components:

- Estimate the aircraft range and autonomy
- Assess the battery state of charge given a flight path
- Size the electric motor and its cooling

In particular, this demo features a serial hybrid design in which a combustion engine powers a generator which then delivers its generated electrical power not only to the propeller via electrical buses but also to a battery connected to the system. Here, there is an image 2.5 showing the actual simulation template before anything is modified.

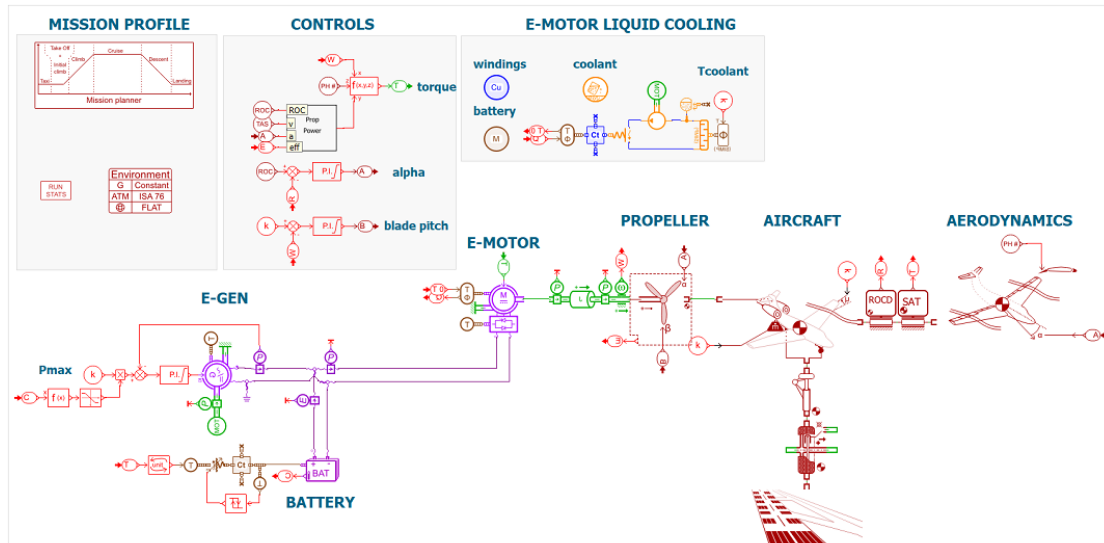


Figure 2.5 - *Original Series Hybrid Template*

As shown, this system is composed of different components, supercomponents (groups of conjoint components), all of which can be customized and personalised. Here are some of the main ones:

(a) Mission profile

This section 2.6 of the program is composed of various components. The first one and most important is the mission planer component, which allow us to draft a flight plan by adding different sections divided into climbing phases, cruise phases and descent phases. Also, it is possible to define the air speed, altitudes, angles and times that each phase has to follow. Finally we get a plot that shows the approximate profile of the flight designed.

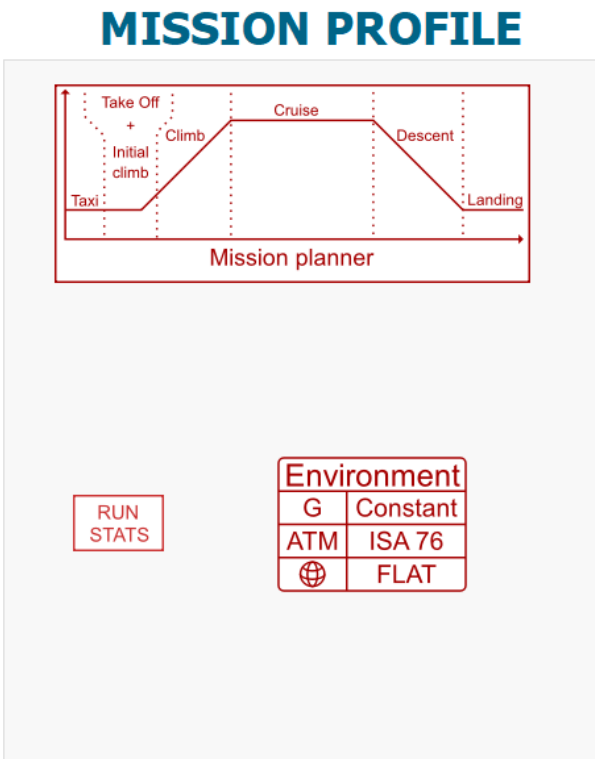


Figure 2.6 - *Mission Profile Section*

In the same section, we can observe the environmental properties generator which allows to define all the information relevant for representing the environment into which the system is evolving. Therefore, the Earth gravity field, the atmosphere model as well as the Earth geometry representation, the starting time of the simulation, UTC time, could be defined in here.

Finally, there is the "Run stats", a component capable of monitoring statistics about the current run such as CPU time used, elapsed time to run the simulation, current integration step...

(b) Controls

This segment 2.7 is specially interesting due to all the parameters and the equations in which they are involved in, represented as a group of signals and controllers.

## CONTROLS

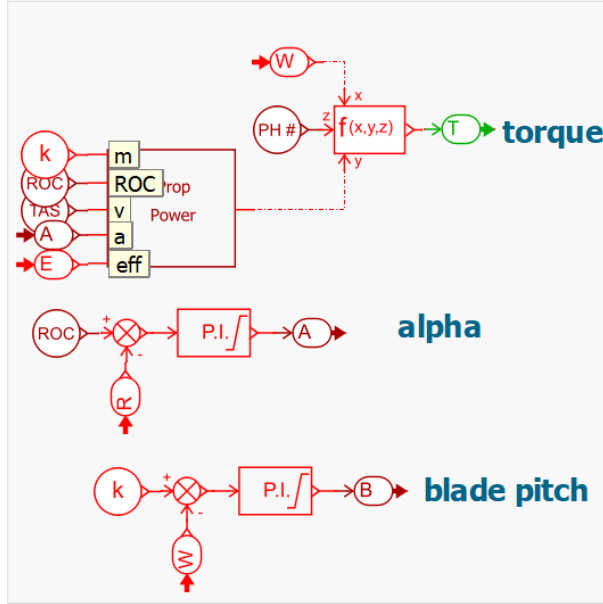


Figure 2.7 - *Controls Section*

Firstly, it is noticeable the components employed to calculate  $\alpha$ , which represents the angle of attack (AOA). The simulations subtracts, from the rate of climb (ROC) given by the flight plan, the actual rate of climb from the airplane to later input that result into a PID controller, which output is like this:

$$v = K_p \cdot u + K_i \int_{t_{start}}^t u dt + K_d \frac{du}{dt} \quad (2.2)$$

Similarly, the angle of blade pitch is calculated as well but in this case, the inputs are different. A constant quantity is used as well as rotation speed of the shaft.

Finally, the first supercomponent of the simulations is used in this section. It takes as input multiple data such as the static air density (SAD), the true air speed (TAS), the efficiency of the propeller, the mass of the airplane, the ROC and the AOA but also, it requires the drag coefficient for each flight phase, which were provided. The component makes use of equations like these:

$$C_L = \frac{2 \times (-\text{thrust} \times \sin(\alpha \times \pi/180) + \text{mass} \times \text{gravity} \times \cos(\sin^{-1}(\frac{\text{ROC}}{\text{TAS}})))}{\rho \times \text{Sref} \times \text{TAS}^2} \quad (2.3)$$

where:

- $C_L$  is the coefficient of lift,
- *thrust* is the thrust force [N],

- $\alpha$  is the angle of attack [degrees],
- $mass$  is the mass of the airplane [kg],
- $ROC$  is the rate of climb [m/s],
- $TAS$  is the true air speed [m/s].
- $S_{ref}$  is the reference surface, the wing surface in our case [ $m^2$ ]

$$thrust = \frac{(mass \times gravity \times ROC/TAS + 0.5 \times \rho \times CD \times S_{ref} \times TAS^2)}{\cos(\alpha \times \pi/180)} \quad (2.4)$$

where:

- $thrust$  is the thrust force [N],
- $C_D$  is the coefficient of drag,

$$power = \frac{thrust \times TAS}{propeff \times N_{eng}} \quad (2.5)$$

where:

- $power$  is the power needed by the aircraft [W],
- $N_{eng}$  is the number of engines in the plane,

Equations 2.3, 2.7, 2.5 give us the actual calculations of the coefficient of lift (CL), the thrust of the plane and the power needed, with which the supercomponent is programmed with.

Once the propulsion power is known, the last equation 2.6 can be used to figure out the torque needed.

$$T = \frac{mg \cdot ROC/TAS + D}{\cos(\alpha)} \quad (2.6)$$

where:

- $T$  is the torque needed to be produced by the aircraft [N],

This signal will later be transmitted to the electrical motor so that it produces the correct amount of rotational moment.

### (c) E-Motor liquid cooling

This part of the simulation can be used as a model for the real cooling mechanism that would take care of the engine's refrigeration 2.8. It is really important to simulate the engine's temperature since an engine overheat could lead to its complete failure which, in case it happened in the midst of a mission, would lead to a extremely dangerous situation an possible loss of control of the aircraft.

## E-MOTOR LIQUID COOLING

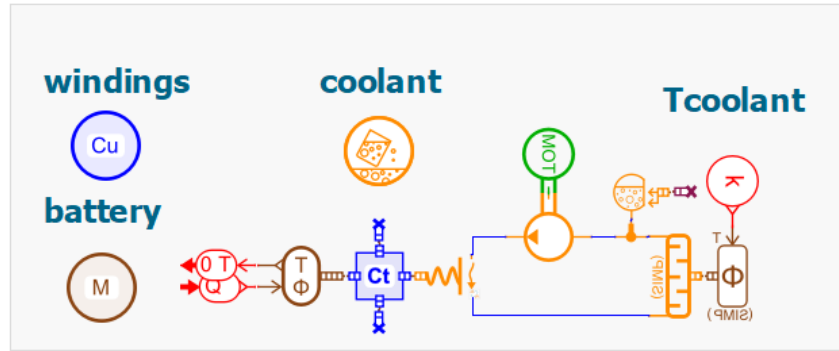


Figure 2.8 - Cooling Section

This system specifies the properties and materials of the battery, the windings and the coolant. Thanks to a pump activated via a small motor and a coolant accumulator, the heat coming from a thermal mass, made from the material already specified, is absorbed by the coolant's current via heat exchange and a convention mechanism.

The input of this small system is the heat flow coming from the electric motor and the output of the system is the temperature signal that feeds the electric motor, as it is shown in the e-motor section.

### (d) Electric Generator

This section of the simulation describes the source of energy that the plane relies on. The electric generator plays a crucial role in the overall propulsion system since it serves primarily to produce electrical power from mechanical energy. In AMESim, the generator essentially functions as an electrical current generator.

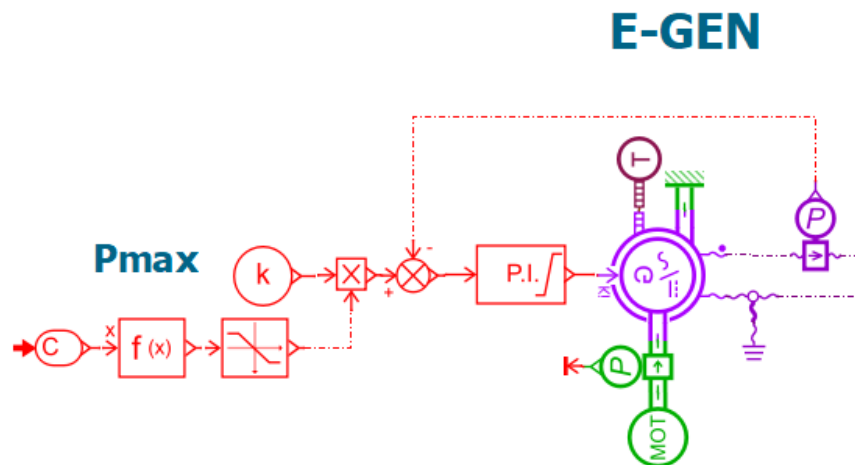


Figure 2.9 - Electric Generation

As we can see in 2.9, the generator component is fed by various signals, the first that comes into view is the control signal (red components). In this case, the alternator

control is designed outside the alternator model itself, which will supply the generator with a signal between 0 and 1. This controller takes into account the state of charge of the battery, the maximum power that the generator can provide and actual power generated which is used in a feedback loop. External controllers and their structure follow the following scheme 2.10:

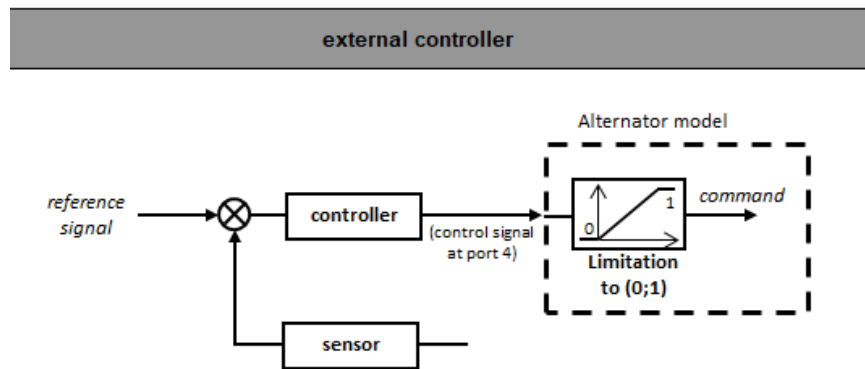


Figure 2.10 - *External controller*

In order to define the alternator, parameters such as the minimum speed for the generator to deliver current as well as for delivering the maximum current and the maximum current itself, have to be established.

Additionally, the alternator necessitates a source of mechanical energy, which, in the context of a hybrid configuration, comes from a combustion engine. To simplify the modeling process, the engine is represented as a constant rpm source, accounting for the practical limitations of the real combustion engine. However, a more intricate model could be implemented for further analysis and refinement.

Finally, a temperature source is installed which symbolises the air that cools down the alternator. It is set at 20°C.

(e) Electric Motor

The fundamental part of this simulation is the electric motor component. It is comprised by the machine, the inverter, the control unit and a sensor 2.11.

# E-MOTOR

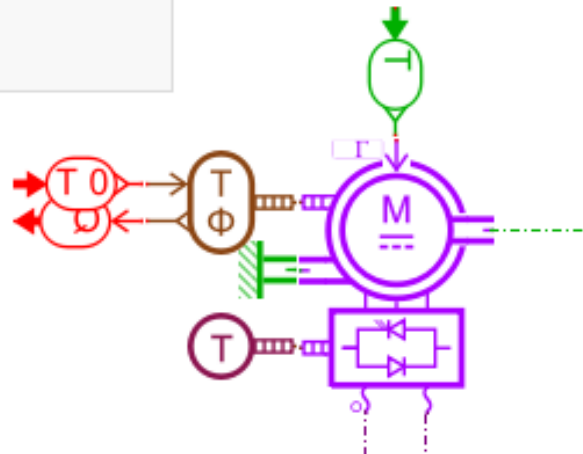


Figure 2.11 - Electrical motor

This model can be simply characterised by defining the efficiency, the maximum power, and the maximum speed of the machine. One crucial advantage of this model is that the machine is reversible 2.12 meaning it can act as a motor or as a generator. Depending on the rotor relative speed, the torque and its respective signs, the machine will work either as a motor that propels the plane or as a generator used to replenish the battery.

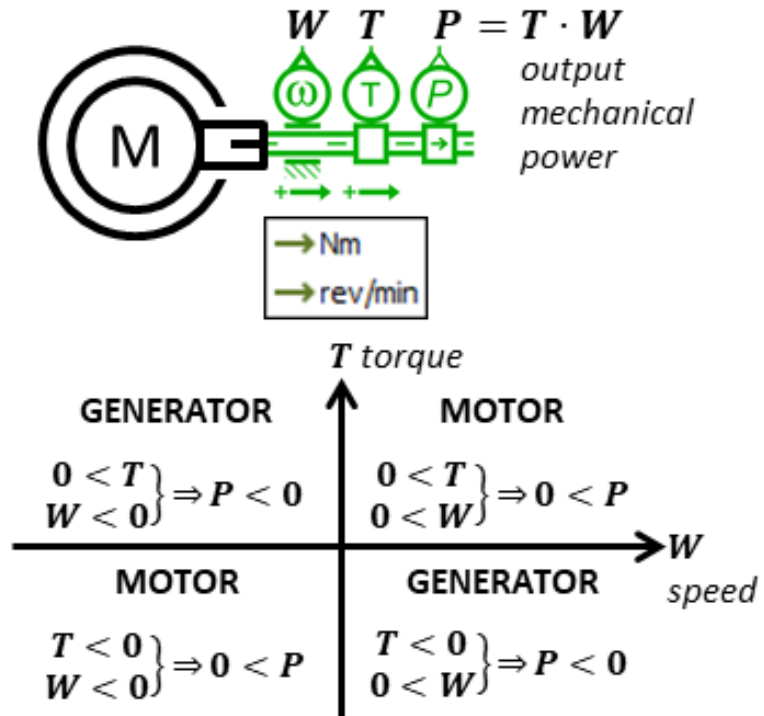


Figure 2.12 - Dual behavior of the model

In this simulation, the component is fed, from the top, by a signal representing the

necessary torque needed by the aircraft as well signals coming from the refrigeration system already explained. This last signals contribute to keeping the actual motor cool enough to maintain its efficiency. The heat flow from the motor is the output and the temperature after the cooling cycle is the input.

The output of the model is directly communicated through another component, which simulates the shaft 2.13, to the aircraft's propeller. Also, the rotating speed of the shaft is sent via dynamic transmitter to the control section so that it can be used to calculate the blade pitch.

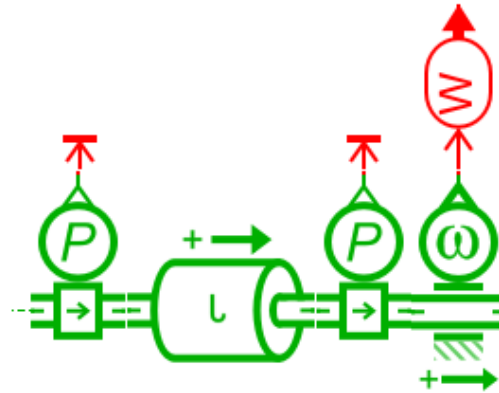


Figure 2.13 - Main shaft

#### (f) Battery

Another vital part for the hybrid design is the battery section 2.43. This subsystem plays a pivotal role in providing electrical power for propulsion and onboard systems. The battery can be charged by either the generator or the electrical motor when it enters its generator state.

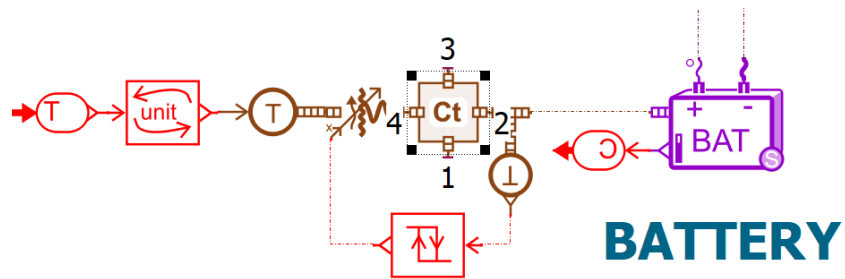


Figure 2.14 - Battery subsystem

As observed, the system sends its state of charge through a transmitter to the control system of the generator so that it allows it to perform its duty, unless it reaches 0% which cuts the signal that feeds the generator so that it cannot function.

A thermal circuit is established as well. It takes as input the static air temperature which is measured in another section of the simulation and comes in kelvin. Thanks to a unit converter, it changes units to Celsius. By using a component that accounts for the forced and free convection, the heat is exchanged between the battery, simulated as a thermal mass made of a predefined material, and the air. Finally, the resulting temperature is an input for the battery component and it is also a signal that, thanks to a sensor and a trigger, establishes the air velocity in the convection.

(g) Propeller

Despite the intended operation of our ultralight aircraft with a rotor/stator propulsion system, the software in use does not allow for the possibility of simulating such a device. Therefore, an approximation must be made to simulate a simpler system, which in this case, it will be a normal propeller 2.15. It will be meticulously modelled to emulate the behavior of the actual propulsion system in order to maximise the accuracy of this simulation.

## PROPELLER

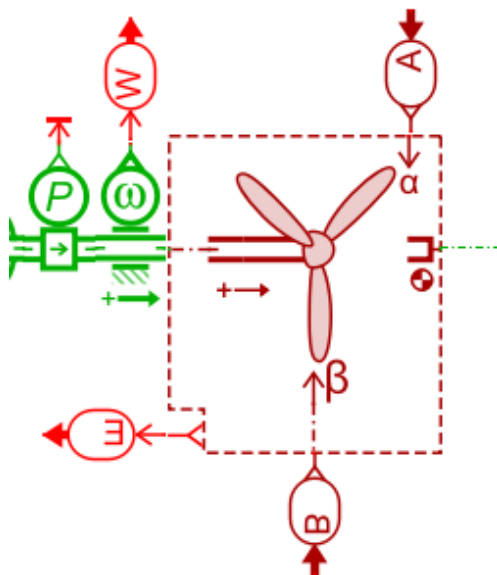


Figure 2.15 - Propeller

The component takes as inputs the angle of attack defined for each flight phase and the blade pitch, calculated in the control section of the simulations. Additionally, it needs to be fed by the shaft with torque and rotational speed and it follows a counter-clockwise configuration which will render a positive power exchange, effectively emulating the behavior of a propeller. The primary outputs of this component are the thrust 2.7, the propulsion power 2.8 and the propeller efficiency 2.9.

$$T = C_T \cdot \rho \cdot \pi \cdot \omega^2 \cdot R^4 \quad (2.7)$$

where:

- $T$  is the thrust [N],
- $C_T$  is the coefficient of thrust,
- $\rho$  is the air density [ $\text{kg m}^{-3}$ ],
- $\omega$  is the angular velocity of the propeller [rev/s],
- $R$  is the radius of propeller [m].

$$P_{\text{prop}} = T \cdot V_a \quad (2.8)$$

where:

- $P_{\text{prop}}$  is the thrust power,
- $T$  is the thrust,
- $V_a$  is the axial aerodynamic velocity of the propeller.

$$\eta_{\text{prop}} = J \times \frac{C_T}{C_P} \quad (2.9)$$

where:

- $J$  is the advance ratio of the propeller [1/rev],
- $C_T$  is the coefficient of thrust,
- $C_P$  is the coefficient of power,

$$J = \frac{V_a xi}{n \cdot D} \quad (2.10)$$

where:

- $J$  is the advance ratio of the propeller [1/rev],
- $V_a xi$  is the axial aerodynamic velocity [m/s],
- $n$  is the angular velocity of the propeller [rev/s],
- $D$  is the diameter of propeller [m].

The propeller can be modeled in different manners. However, the one which can allow for a more detailed configuration is by creating a table for properties such as the coefficients of power and thrust. Via this tool, it is possible to both design a propeller using its geometric characteristics and compute the performance map of the propeller using Blade Element Momentum Theory.

## (h) Aircraft

This section of the simulations gathers multiple components which simulate various parts of the plane's body.

The first and most notable component is used to model a point mass moving through space whose mass varies with time, as a consequence of the consumption of fuel. It also is employed to keep track of the aircraft's linear velocity and its location.

## AIRCRAFT

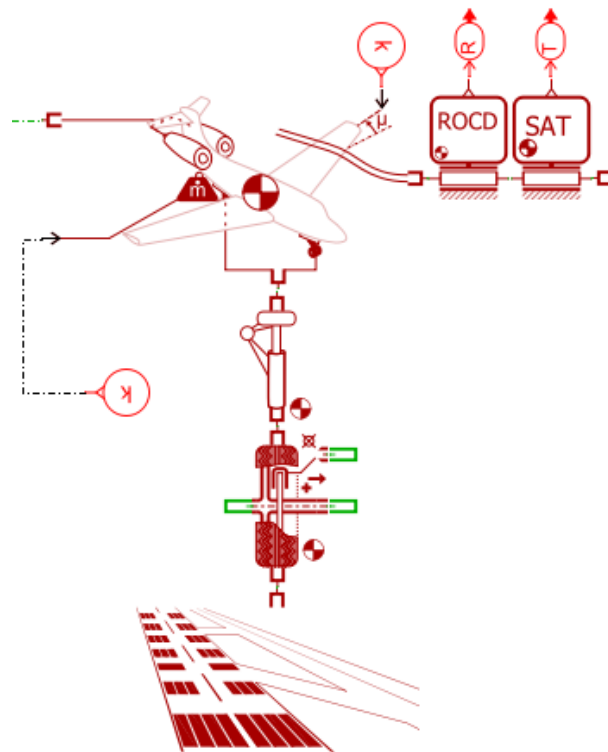


Figure 2.16 - *Aircraft*

Just below the point mass component, the aircraft's suspension is modelled as an analogy with a mass-spring-damper system 2.17. The suspension efforts are generated by a vertical and a longitudinal suspension and, when connected to an aircraft body and tire, the vertical suspension primarily counters weight forces, while the longitudinal suspension counters tire-generated efforts. This component is useful to study flight phases such as taxiing, take-off and landing where point mass assumptions are valid.

Furthermore, two sensors are integrated with this component, facilitating the measurement of the rate of climb and static air temperature. These quantities are sent through transmitters to other parts of the simulation, specifically, the control sections. The rate of climb data can be utilized to derive the angle of attack, whereas the static air temperature plays a major role in the regulation of the battery's cooling mechanism.

Finally, the tire and the runway constitute the final two components. The tire component computes the forces developed by our actual wheel during the aforementioned phases. Among the many parameters that this component handles are the angular velocity of the wheel, the torque experienced, the position, velocity and acceleration of the axle and in addition to various other data sourced from the runway.

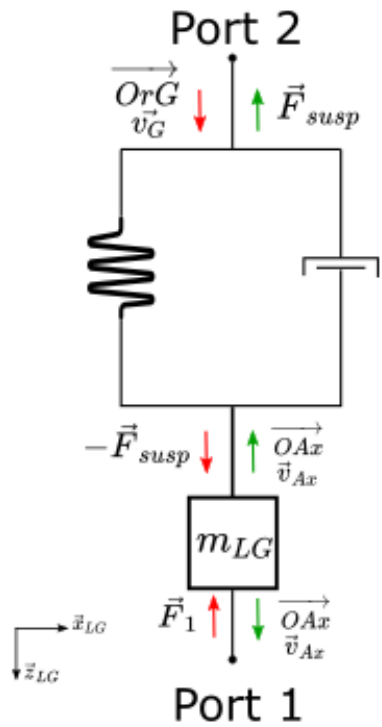


Figure 2.17 - Suspension's analogy

(i) Aerodynamics

In addition, one fundamental component in the simulation is the one that imposes global aerodynamic efforts suffered by the plane under point mass assumptions 2.18.

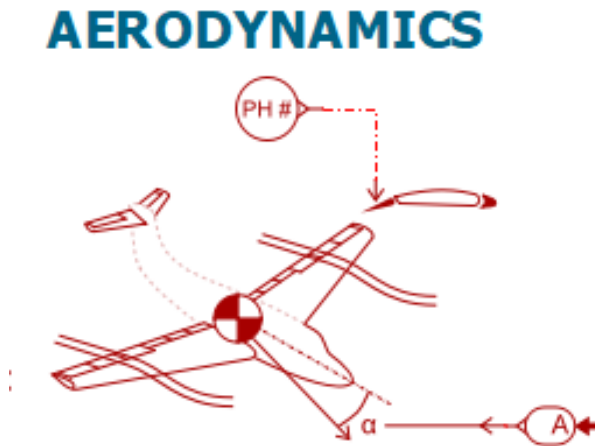


Figure 2.18 - Aerodynamic forces

The primary inputs for this component consist of equations governing the coefficients of lift and drag, which are often defined through tables exhibiting various forms depending on the amount of parameters taking into account for the calculation. Typ-

ically, when enough data is available, the tables can express the already mentioned coefficients as a function of the angle of attack, the Mach number, the altitude and in the case of the coefficient of drag, the coefficient of lift is also necessary.

Nevertheless, for simplicity purposes, the coefficients of lift will be inputted as a function of solely the angle of attack ( $\alpha$ ) via a simple 1D table. The designer firm offered values calculated by the use of specialised software such as ADS and those will serve to figure out the equations for the coefficient of drag. This way, all the parameters will be related to the one that we were provided with. Specific calculations will be explained later on.

Additional inputs required by this component include the angle of attack, which plays a critical role in determining the coefficients' behavior and the flight phase as well, enabling the component to select the right configuration.

This component makes use of the following equations to calculate the forces of lift 2.11 and drag 2.12, which are commonly used in the aviation design field [25]:

$$F_L = \frac{1}{2} \cdot C_L \cdot \rho \cdot A \cdot TAS^2 \quad (2.11)$$

where:

- $F_L$  is the lift force,
- $C_L$  is the coefficient of lift,
- $\rho$  is the air density,
- $A$  is the reference area (such as wing area in our case),
- $TAS$  is the true air speed.

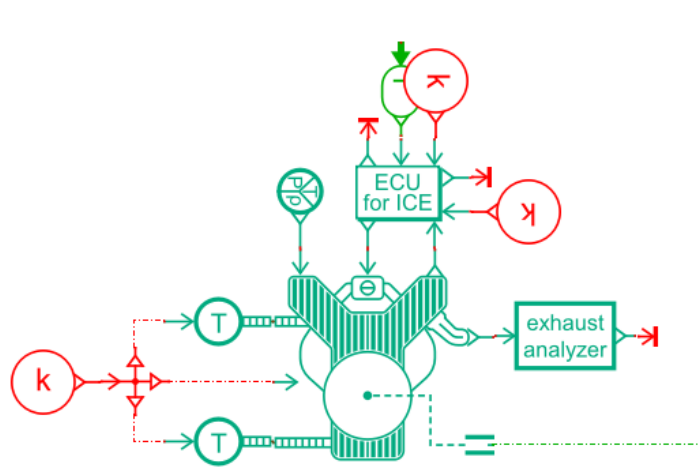
$$F_D = \frac{1}{2} \cdot C_D \cdot \rho \cdot A \cdot TAS^2 \quad (2.12)$$

where:

- $F_D$  is the drag force,
- $C_D$  is the coefficient of drag,
- $\rho$  is the air density,
- $A$  is the reference area (such as wing area in our case),
- $TAS$  is the true air speed.

#### (j) Internal Combustion Engine

Next, a vital section of the model is the conventional gasoline engine 2.19. In this case, we will be using the Rotax 912 Ultra Light engine, a four-stroke, horizontally opposed, four-cylinder engine. We will discuss its characteristics later.



## ROTAX 912 UL

Figure 2.19 - Engine by Rotax

This component is used whenever an engine performance over a cycle is required and it can accurately predict the fuel consumption and emissions over driving cycles by using low CPU capacity. This mechanism works by supplying the software with tables of data that characterise the way the engine works.

The component requires data belonging to the outside air, the temperatures which result from losses from the combustion and the friction itself, and most importantly the ECU unit. The Engine Control Unit is fundamental for the right performance of the engine because it is tasked with ensuring the right communication between the pilot request and the engine control signals.

Finally, a component that can theoretically predict the amount of pollutants produced during the cycle and emitted to the atmosphere was included, thus it is possible to compare this design's environmental impact to other similar planes, other engine selection or even other hybrid configurations.

### (k) Micro Turbine Generator (MTG) unit

As it was petitioned, another way of generation of power will be studied and included in this report, which can be used instead of the combination of ICE plus generator. This generation unit will be based in a model called TurboGenerator 2.20, a creation by Turbotech which is a french based company. Originally, it was founded by engineers and members of Safran Aerospace but the mission of this enterprise is to deliver solutions based on new generation of high-performance turbine-engines and enable long range hybrid flights. Their objective is to achieve technological dominance over aeronautical propulsion solutions for both hybrid and conventional aircraft.

## TurboTech TurboGenerator

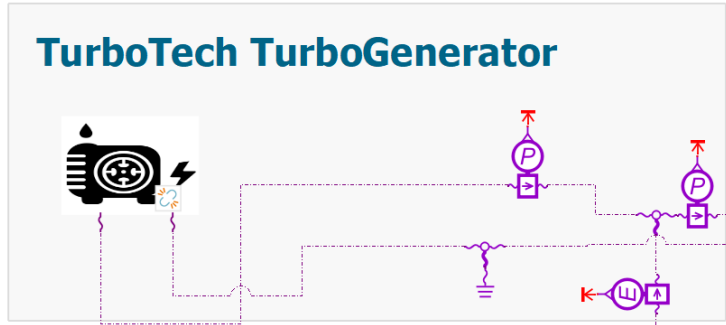


Figure 2.20 - *TurboGenerator* by *TurboTech*

Since the whole unit follows a Brayton cycle, it does include all the components belonging to such a cycle like the compressor, the combustion chamber, the turbine, the generator and the most important part, the recuperator, which is a heat exchanger connecting the current of exhaust gasses and the air leaving the compressor. Dealing with all these submodels would be extremely confusing and distinguishing them from the rest of the model would be quite annoying. Therefore, the entirety of the model will be confined inside a supercomponent.

The main problem with using classical turbomachines and Brayton cycles is that the default and primary strategy to designed them for ULM is to scale down the existing models for bigger and heavier aircraft [26]. However this leads to extremely poor fuel efficiencies of only around 10%. This is the main reason of why there is not that many small turbines in the market and piston engines are the preferred solution for light aviation. Also, the fact of having a better and cheaper alternative leads investors to bet for already known technologies rather than risking contributing to turbine development.

TurboTech has found the solution for the problem previously mentioned. By the usage of tools like CFD, CAD and CAE through ANSYS and CATIA, they managed to engineer a heat exchanger working as a recuperator which not only makes use of energy which otherwise would be wasted but also greatly lowers the consumption of fuel and increases the range at the cost of a slightly bigger volume. This invention is so revolutionary that TurboTech has a patent on it. Regarding at [11], the exchanger is described as a set of various cases and some can contain about 2000 small tubes with a length of 300 mm, an inner section of 2,8 mm and an outer section of 3 mm.

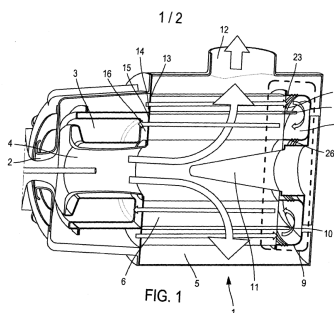


Figure 2.21 - *Half cut of TurboGenerator*

### 2.1.3 Existing models

As mentioned before in this report, some efforts have been made to further advance in the fields of electric aviation. Big corporate enterprises have come up with different designs to approach the challenges that lie within the concept of hybrid airplanes. We will take a look at the ways these companies have developed their models.

- eFlyer from Bye Aerospace [8]

The eFlyer program was created by the American company Bye Aerospace with the objective of developing a 2 seat electric training aircraft. The first result of the program was the eFlyer 2.

It became the world's first FAA 14 CFR Part 23-Type Amendment 64-Certified Applicant for a "Normal Category" Electric Aircraft featuring a completely structure with almost twice the average aerodynamic efficiency of other aircraft of similar size. The plane employs an electrical ENGINeUS 100 motor in tractor configuration, developed by the known French company Safran, which is capable of generating 150 HP or 110 kW.

Besides, the plane will feature up to six high energy density lithium battery, a Toray carbon composite structure and the avionics will follow the G500 TXi model designed by Garmin.

Some of the capabilities of this model are:

- (a) 450 lb of payload (crew included)
- (b) 1200 ft/m max rate of climb
- (c) Speeds ranging from 55 to 135 knots
- (d) Flight endurance of 3 hours (at 73 knots)
- (e) Maximum altitude of 14000 ft

- E-Fan by Airbus [1, 3]

The E-Fan project began during the 2011 Paris Air Show, as a successor project for the CriCri 2.22 and the project was officially launched in October of 2012. It became a collaborative effort between Aero Composites Saintonge (ACS) and Airbus and the first version was presented in the 2013 Paris Air Show.



Figure 2.22 - *Cricri by Airbus*

As the program advanced, the development of the E-Fan 1.0 came to fulfilment. This model corresponds to a 1 seat training experimental aircraft that, at the beginning, was completely electric, but from 2016 forwards, several attempts to include a hybrid design were performed (Solo 2526 thermal engine for the E-Fan Plus). The plane sports a power plant consisting of 2 electric motors of 30 kW each and two ducted fans which enhance the static thrust, reduce the perceived noise and improve the safety on the ground. All this machinery is powered by a 167 kg 250V lithium-ion polymer battery pack manufactured by KOKAM.

Several facets of proficiency within this model are:

- (a) MTOW of 550 kg
- (b) Max speed of 220 km/h
- (c) Cruise speed of 160 km/h
- (d) Flight endurance of 45-60 minutes
- EcoPulse by Airbus [5, 6, 4]

EcoPulse 2.23 is a distributed hybrid-propulsion demonstrator aircraft developed by Airbus in partnership with Daher and Safran unveiled in the 2019 Paris Air Show.



Figure 2.23 - *EcoPulse*

It consists of a modified Daher TBM 900 turboprop aircraft which has been greatly altered to sport, apart from its standard and propeller systems, six wing-mounted propellers, each of which is driven by a 50-kW Safran ENGINeUS electric engine powered by a Power Distribution and Rectifier Unit (PDRU) supplied by Daher.

Besides, the demonstrator is equipped with a customized battery designed and developed by Airbus Space and Defense. Unlike those from hybrid cars or other aviation modes, this one is a high voltage battery able to achieve 800 Volts DC and deliver up to 350 kW of power, thus capable of supplying the 6 small propellers.

The main reason for this plane's existence is the possibility to assess the performance impact of having a distributed propulsion system and a new hybrid design to further develop a mix of solutions to support the transition to low-carbon aviation, which is the main aim of of Airbus' decarbonisation roadmap.

## 2.2 Design of airplane's frame

The aim of this project is to create a plane which allows the passenger to enjoy the views of the landscape as he/she profits from a special vantage point above the skies. To achieve this, the plane must meet several requisites:

- Maximum visibility
- Economical flight hour and energy optimization
- Attractive design and noise reduction
- Safe design and air-conditioned cabin

Indeed, these are quite ambitious objectives although, the most restrictive is that the frame and the overall design of the plane must remain within the Ultra Light aircraft (ULM) category or the Light Sport Aircraft (LSA in the United States). We will discuss what these categories imply in depth in another section of the report.

Besides, some other important specifications of the plane will be:

- (a) Mindus-DP-V1 2.24 frame will be the chosen design for the fuselage and the overall architecture of the plane
- (b) Hybrid propulsion system in series configuration consisting on a ICE (Rotax 912 UL) powering a generator that will supply an electrical motor used to generate torque for a ducted fan system 2.25 as well as battery
- (c) Retractable tricycle landing gear 2.26 and swept wing
- (d) V-shaped tail

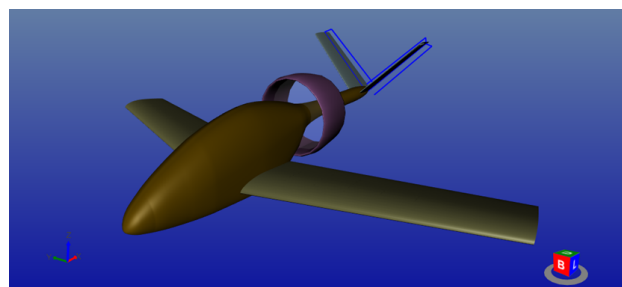


Figure 2.24 - *Mindus V1 by AOD*

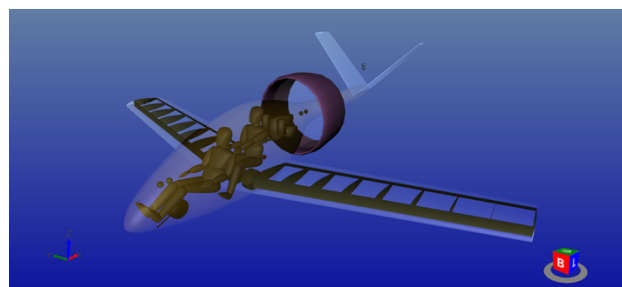


Figure 2.25 - *Interior and ducted fan of Mindus V1*



Figure 2.26 - *Extended landing gear of Mindus*

### 2.2.1 Ultra light aircraft definition - Weight of the plane

As mentioned in the previous section, the design corresponds to an ULM, which is a way to classify airplanes depending mostly on its weight. The European Union imposes many regulations through the European Union Aviation Safety Agency (EASA) [2] which has been a central authority in aviation safety and environmental protection in Europe for over 20 years. EASA is responsible for adopting rules across all aviation fields, certifying and approving products and organizations, providing oversight and support to Member States and promoting the use of European standards.

The EASA, in collaboration with the French Ultralight Federation (FFPLUM), defined a category called Ultra Light Motorised, featuring light, easy to handle and recreational aircraft that offer an accessible and economical means for individuals to enjoy flying. These sort of designs were regulated by the 1998 ULM decree [12] which stated that the maximum weight they could reach was 450 kg, including weight bonuses in case of installation of a safety parachute or use on water.

The FFPLUM decided to implement some changes in their newly regulation published decree of June 24, 2019. The aim of this French organization was to support the ultralight aviation usage by expanding its possibilities within limits compatible with a safe regulatory framework allowing aviation practice accessible to a greatest number of enthusiasts. In order to accomplish this, they increased the maximum weight of ultralight airplanes and helicopters to 500 kg, which compared to the former lighter limit, relieves the constrains of many designs.

The following table 2.1 explains the new weight limits on each category of aircraft, as it has officially been published in [24].

	Classe 1 paramoteurs	Classe 2 pendulaires	Classe 3 multiaxes	Classe 4 autogires	Classe 5 dirigeables	Classe 6 hélicoptères
monoplace	monoplace	monoplace	monoplace	monoplace	monoplace	monoplace
Masse maximale (kg)	300	300	330	330	1200 m <sup>3</sup> air chaud 400 m <sup>3</sup> autre gaz	330
Puissance maximale (kW)	60	60	65	85	2000 m <sup>3</sup> air chaud 900 m <sup>3</sup> autre gaz	85
Vitesse de décrochage (km/h)	-	65	70	-	-	-
biplace	biplace	biplace	biplace	biplace	biplace	biplace
Masse maximale (kg)	450	450	500	500	500	500
Puissance maximale (kW)	75	75	80	105	105	105
Vitesse de décrochage (km/h)	-	65	70	-	-	-

(1) + 15 kg si parachute pour les classes 1 à 4 et 6, + 30 kg si utilisation sur l'eau pour les classes 2, 3, 4 et 6 (cumulables)  
(2) + 25 kg si parachute pour les classes 1 à 4 et 6, + 45 kg si utilisation sur l'eau pour les classes 2, 3, 4 et 6 (cumulables)

Table 2.1 - *New limits for the 6 classes of ULM*

According to the new weight limitations, the design supplied by OAD must adhere to specific threshold values such as a maximum weight of 500 kg plus an additional +25 kg due to the installation of a parachute. Other important considerations would be:

- (a) Maximum Take Off Weight (MTOW) of 530 kg
- (b) Empty weight of 341.3 kg
- (c) Useful weight of 189.2 which consists of a payload of 156 kg and 33.2 kg of fuel
- (d) Fuel consumption and thus weight decrease needs to be computed

## 2.2.2 Geometry

The company tasked with the design of the plane is Optimal Aircraft Design (OAD) [29]. This company is also responsible for programming and developing ADS, a comprehensive yet compact software that enables even inexperienced engineers to create and model their own designs.

The airplane is intended to be constructed from lightweight aluminum alloys and carbon fiber to optimize aerodynamic performance, stability, and weight. The design aims to be simple and easy to handle. The geometric parameters will reflect the aircraft's aerodynamic characteristics and overall design philosophy.

### General measurements of the Mindus

- Overall length: 6.585 m
- Overall height: 2.538 m
- Wingspan: 7.979 m
- Wing area: 9.095 m<sup>2</sup>
- Wing Airfoil : NASA-NLF(1)0416
- Horizontal Tail span: 2.625 m
- Horizontal Tail area: 3 m<sup>2</sup>
- Tail Airfoil: NACA-0009
- Root chord: 0.951 m
- Tip chord: 0.665 m
- Fuselage length: 6.331 m
- Fuselage mean diameter: 1.104 m
- Fuselage wetted area: 12.805 m

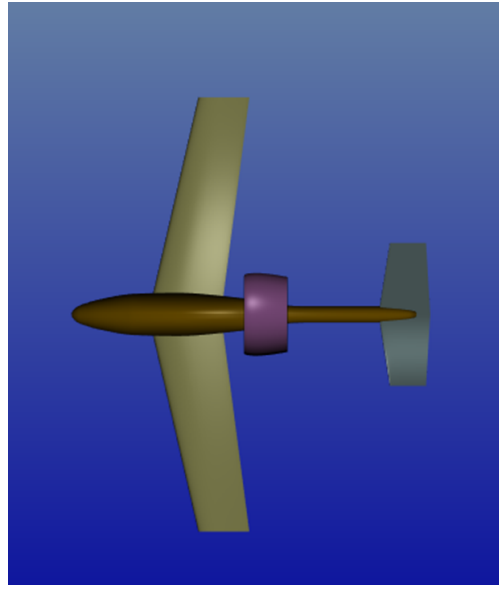


Figure 2.27 - *Upper view of Mindus*

## 2.3 Internal combustion engine

For the hybrid design, it was decided that a traditional Internal Combustion Engine should be employed instead of other alternatives such as fuel cells.

An ICE is a type of engine where fuel is burned within a confined space in which the expansion of high-temperature and high-pressure gases produced by the combustion process is used to directly move a piston (like in our case) or turbine blades generating mechanical work and propulsion. However, the usage of a ICE in aviation is quite different from other applications because numerous additional factors must be considered. Obviously, choosing an engine for an aircraft involves different criteria compared to selecting an engine for a conventional car.

Some parameters that have to be deeply considered for choosing the right option of engine are:

- (a) Power output: the engine must provide sufficient power to meet the aircraft's performance requirements during each phase.
- (b) Weight: the engine is one of the main contributors to the total weight of the plane.
- (c) Fuel efficiency: fuel consumption is crucial for range and operating costs.
- (d) Cooling requirements: adequate cooling is essential to prevent engine overheating and engine failure.
- (e) Noise and emission: regulations and laws regarding these factors may influence the selected engine.

By evaluating these parameters, aircraft designers and operators can select the most suitable ICE for their specific application.

### 2.3.1 Rotax: engines and applications

Rotax Aircraft Engines, originally established in Dresden, Germany, in 1920 [20], relocated to Austria in 1943. The majority of Rotax shares were taken over by the Vienna-based Lohner-Werke in 1959 and in 1970, Lohner-Rotax was bought by the Canadian Bombardier Inc.

As the brand's name suggest, this company focuses on the developments and production of light internal combustion engines. These engines are a popular choice within the aviation industry, particularly for light aircraft, ultralight aircraft, and light-sport aircraft (LSA). Also, their engines can be used for much more than just airplanes.

Some of the less known uses for Rotax engines are:

- Snowmobiles
- Personal watercraft
- Off-road vehicles
- Karting

The company has created various models of engine [19] which differ in size, capabilities, consumption and power output:

- Rotax 916 IS A (160 hp) 2.28: Dynamic, turbocharged iS engine with best power-to-weight ratio and TBO 2,000h



Figure 2.28 - *Rotax 916 IS A*

- Rotax 912 IS Sport (100 hp) 2.29: Perfected 4-stroke engine with full take-off power and engine management system



Figure 2.29 - *Rotax 912 IS*

- Rotax 915 IS A (141 hp) 2.30: Dynamic iS engine with best power-to-weight ratio



Figure 2.30 - *Rotax 915 IS A*

- Rotax 912 ULS (100 hp) 2.31: Engine with the best-in-class power-to-weight ratio



Figure 2.31 - *Rotax 912 ULS*

- Rotax 914 UL (115 hp) 2.32: Low-weight engine with excellent performance at high altitudes.



Figure 2.32 - *Rotax 914 UL*

Even though Rotax has many more products to offer, these are the most relevant and related to the project. However, the study and observation of the different engines and their capabilities produced by Rotax and the areas in which the company itself has experience, will serve as a base to select the final power source which best fits the prototype.

In the following sections, the most adequate machine for the power plant will be selected and explained.

### 2.3.2 Rotax 912 UL

After much deliberation, there is one engine which best fits our model and does out-perform every other according to our criteria that has been mentioned in other sections. This engine is no other than the Rotax 912 UL 2.33 2.34.



Figure 2.33 - *Rotax 912 UL*



Figure 2.34 - *Rotax 912 UL*

The Rotax 912 UL is a commonly used engine for light aviation that out-stands due to its high reliability and good power-to-weight ratio. It was first sold in 1989 and first approved for certified aircraft in 1995, and from that point onwards, it has been used in many designs such as the Pipistre Vitus SW 80 2.35 and many other famous planes. It even became one of the most sold aircraft engines in 2014, when a total of 50000 units were sold.



Figure 2.35 - *Virus SW 80 by Pipistrel*

Concretely, the Rotax 912 UL is a horizontally opposed 4 piston engine with 4 liquid and air cooled cylinders. It features a system of spark ignition, dry sump forced lubrication with separate oil tank, automatic adjustment by hydraulic valve tappet and 2 carburetors. All this while it remains the lightest engine in the Rotax portfolio, standing at a base weight of 55.4 kg, although this quantity can be increased if other components are taken into consideration like the exhaust system, the overload clutch etc. This engine is capable of:

- Producing up to 59,6 kW or 80 hp at 5800 rpm during take off
- Supplying a steady quantity of 58 kW at 5500 rpm as continuous performance
- Outputting a maximum of 103 Nm at 4800 rpm

The Rotax 912 UL features a top speed of 5800 rpm which can sustain for about 5 minutes, thus is intended for take off, a maximum continuous speed of 5500 rpm and an idle speed of around 1400 rpm. The tables 2.36, 2.37, and 2.2 extracted from [21], present the performance of the engine as a function of the engine speed as well as its fuel consumption:

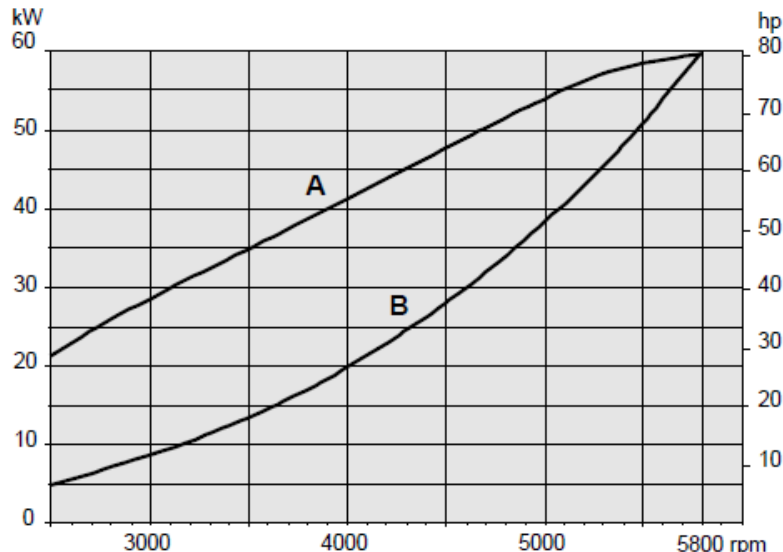


Figure 1: Performance graphs 912 A/F/UL

A max. engine output      B power requirement of propeller

Figure 2.36 - Performance of the Rotax 912 UL

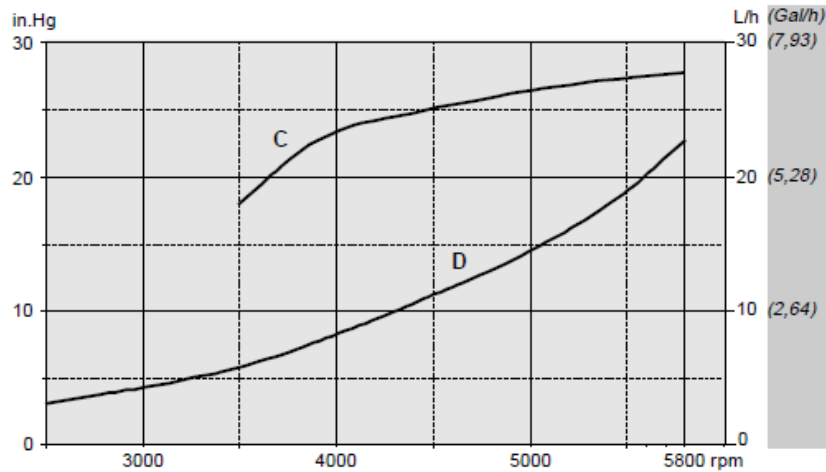


Figure 2: Values along propeller curve

C manifold pressure

D fuel consumption

Figure 2.37 - Consumption of the Rotax 912 UL

Power setting	Engine speed (rpm)	Performance (kW)/(HP)	Torque (Nm)/(ft. lb)	Manifold pressure (in. Hg)
Take-off power	5800	59.6 / 80	98.1 / 72.35	full throttle
max. continuous power	5500	58.0 / 78	100.7 / 74.27	full throttle
75 %	5000	43.5 / 58	83.1 / 61.29	27.2
65 %	4800	37.7 / 50	75.0 / 55.32	26.5
55 %	4300	31.9 / 43	70.8 / 52.22	26.3

Table 2.2 - Rotax 912 ULS Performance Specifications

Some technical data about the engine was required for the simulation so that the proper maps and tables can be generated by AMESim. The software has some tools and is capable of developing its own tables for power, consumption and emissions if enough data is provided:

- Bore: 79.5 mm
- Stroke: 61 mm
- Displacement: 1211 cm<sup>3</sup>
- Compression ratio: 9

These last parameters are important for correctly calculating the performance of the engine since higher displacement volumes and higher compression ratios point towards greater thermal efficiencies, meaning more energy is extracted from the fuel. Moreover, capitalizing on the reference to fuel, it is worth mentioning that this type of engine can run on various sources of energy. Firstly, the Rotax 912 UL may run on MOGAS, especially, the European standard EN 228 normal, super and super plus. However, for performance

reasons, another fuel will be selected. It is the AVGAS 100LL, a fuel quite commonly used for small aircraft which, thanks to its low lead content, has a higher octane number and allows for higher temperatures and pressures before detonating that ultimately results in greater thermal efficiency.

## 2.4 Generator

Following the series hybrid configuration, the next important component to model would be the electrical generator. This machine is used as a receiver for the mechanic work produced by the ICE.

It is crucial to correctly select which unit of generation to use since it will produce the power, not only to supply the electric motor and thus the ducted fan as well, but also to charge the battery. Recharging the battery during the flight is a great way to extend the period of autonomy and allow for longer trips. This possibility might even mean the difference between an accident and saving a life, since in case of a complete engine failure, a recharged battery can still supply the rest of the plane and perform an emergency landing. Therefore, it represents a huge increment in the security and flight readiness.

In order to correctly decide how to model and choose an adequate model for our generator, some parameters to keep a close eye on would be:

- Power density
- Weight
- Right speed range

### 2.4.1 Safran: leaders in electrical propulsion

Before choosing the following models for the rest of the missing components of the model, let's take a look at one distributor that is specialized in electrical propulsion of aircraft and helicopters.

This enterprise is none other than Safran [31]. This French conglomerate and company were born in 2005 when 2 other companies, also French, called Snecma and Sagem merged. Both of these companies and many others had a long history expanding from the beginning of the 20th century and were specialized in aviation engines and other aircraft equipment. The group specialized in aerospace, defense and security and from that point on, it has been involved in renowned projects such as the "Clean Sky" in 2008 and "Clean Sky 2" in 2014, both were Joint Technology Initiative which were financed by the European Commission and the European aerospace industry to develop cleaner and quieter aircraft's. Besides, they have worked with other giants of the industry like Airbus in joint ventures like named Airbus Safran Launchers in 2014.



Figure 2.38 - *Safran's Logo*

Seeing that this company accounts for an extensive history in the industry which points towards their high quality and competitive ingenuity, the reliability of their products as well as their specifications and studies done on them, will remain assured. Another great advantage of working with Safran is their great network and influence in the European market, not to mention that there is a delegation in the actual city of Liège. Nevertheless, our attention is particularly directed towards one specific department within this group: Safran Electrical and Power. This entity is a significant contributor in the field of electric and hybrid propulsion equipment. The company specializes in designing and delivering modular, innovative, and optimized architectures and solutions 2.39 which can and will be extremely useful for the simulation.

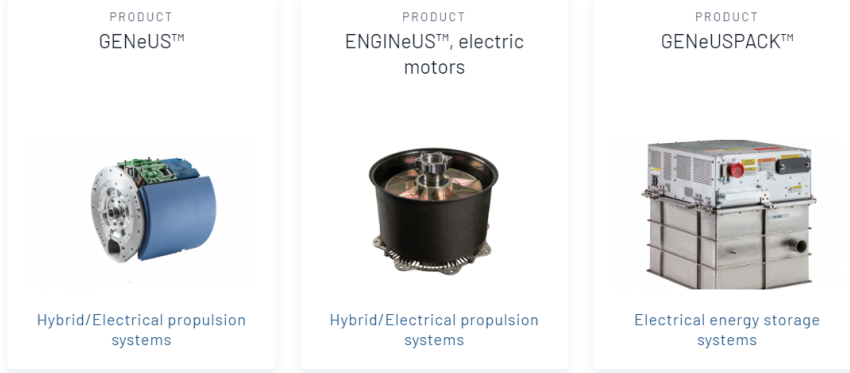


Figure 2.39 - *Safran's products*

## 2.4.2 GENEUS

The GENEUS is the first product of a new family of machines developed and produced by Safran Electrical and Power [18]. It consists of a smart high speed generator with a rectifier capable of producing a controlled DC current and continuous electrical power generation capability of 300 kW. This is the specific case of the GENEUS 300 2.40, which has been tested multiple times by Safran Aircraft Engines and Safran Helicopter Engines, and it has achieved an impressive efficiency of 96%.

After numerous trials, one of which was successfully completed a 500-hour ground test campaign [32], it was determined that this generator is able to reach power density of around 10 kW/kg. This quantity is paramount since the power-to-weight ratio of any machinery or turbo machinery destined for aviation purposes needs to be as high as possible.

These characteristics, added to the relatively low weight of the GENEUS at 30 kg and its compactness make it a very advantageous component for any hybrid design. Furthermore, this machine can even switch between generator and motor mode, although for this project, a different model for an electric motor will be considered.

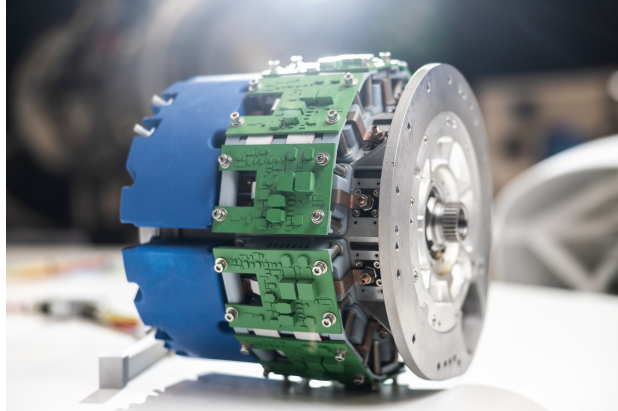


Figure 2.40 - *GENeUS 300 electric generator*

## 2.5 Electrical motors

Next up, there is a paramount part of the series model and that is the electric engine. The integration of electric engines in hybrid aircraft presents several technological advancements and environmental benefits, positioning it as a critical development in modern aviation. Some of the benefits would be:

- Reduced Emissions: when relying on electric power, hybrid airplanes can cut greenhouse gas emissions.
- Noise Reduction: electric engines operate more quietly than conventional engines, leading to reduced noise pollution.
- Improved performance: electric engines provide instant torque and high efficiency across a range of operating conditions.
- Optimized Fuel Consumption: electric engines and their configuration may reduce the consumption of fuel by taking over during some flight phases and relying only on the battery.

### 2.5.1 ENGINus 100

Once again, Safran has devised a solution to another area of the hybrid design. The ENGINeUS 100 is an advanced electric propulsion system developed and produced by Safran Electrical and Power. It has been designed to meet the demanding requirements of modern aircraft, especially of light aircraft.

The ENGINeUS motor family 2.42 offers a range of power outputs from 50 to 1 MW and they integrate an electronic control system into the machine, with an optimized cooling system. The ENGINeUS™ 100 motor is the intermediate model in the range. This one will be the one in which the model will be based on.

Safran's ENGINeUS 100 covers the 100-180-kW range with a power density of 5 kW/kg at peak output [28]. The motor is air cooled, with an embedded motor controller so that it simplifies the aircraft size and minimizes electromagnetic interference. For this model, the speed ranges from 2,500 - 3,000 RPM (continuous power) to 3,500 RPM (peak power).

The power density counting with a integrated motor controller ranges from 3,5 kw/kg (continuous power) to 5 kW/kg (peak power) [17]. The voltage ranges up to 800 V of DC current.

VoltAero's prototype, the Cassio 330 2.41, will utilize Safran Electrical and Power's ENGINeUS 100 smart electric motor in the aircraft's parallel electric-hybrid propulsion system. Thus, it has been proven that this exact type of electric motor can be used for hybrid aviation

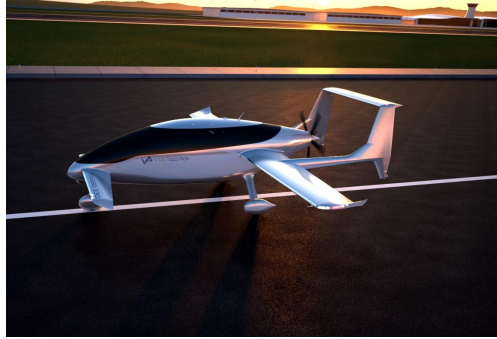


Figure 2.41 - *Cassio 330*



Figure 2.42 - *ENGINeUS 45 for Cassio 330*

## 2.6 Battery

Selecting a battery is another step for the completion of the design because it has major repercussions on the performance, the efficiency and most importantly, the safety of the plane. The choice of including a battery in the plane greatly amplifies its range capabilities as more energy can be stored to freely maneuver the aircraft without having to land back at the airfield to refuel.

Once again, calculating and selecting the right model of battery is crucial for the success of the project but quite different of how this procedure should work in the case of a car.

When working on a aircraft, certain factors gain great importance in this field. Some of the parameters would be:

- (a) Energy density: as it has been mentioned before, this parameters quantifies the amount of energy that can be stored inside a certain amount of mass or volume. The more the battery weights, the lower the range of the aircraft.
- (b) Power density: similarly to energy density, the parameter signifies the amount of power per unit of mass. High power density enables the battery to deliver large amounts of power quickly, quite useful for flight phases like take off.
- (c) Weight and volume: if a battery unit is too big or too heavy to allow for a profitable and safe design, the model must be scrapped. Also, they must comply with weight limitations
- (d) Life cycle: it is the number of complete charge-discharge cycles a battery can undergo before its capacity falls below a specified percentage. The longer it is, the less maintenance and replacement that the plane will undergo.
- (e) Charging time: faster charging times would mean more flights and more customers per day and in return, larger revenues. This must be carefully balanced so as not to risk the battery's health.

### 2.6.1 Safran: power storage and the GENEUSPACK

Safran has been advancing their "battery pack" technology by integrating the highest quality cells available on the market with their own thermal, electronic and mechanical systems and devices. The final result of all these efforts has culminated in the creation of the GENEUSPACK 2.43 battery unit. Even though all aircraft carry small batteries to initiate their engines, Safran's mission is to create a battery which can sustain the propulsion system of the plane. This has been possible due to the acquisition of Zodiac Aerospace by the group and their advancements in lithium-ion technology.



Figure 2.43 - *GENeUSPACK*

Overall, the creation of batteries for the field of aviation brings along 2 different challenges [16]:

- Ensure high cell performance through the right chemical compounds and bonds
- Monitor safety, specifically minimizing the possibilities of thermal runaway which, unfortunately, are directly proportional to the performance

The GENeUSPACK is the result of trying to overcome this challenges and the collaboration between enterprises such as Cuberg. Their lithium metal cell technology has enabled to achieve a specific energy of 280 Wh/kg and an energy density of 320 Wh/L in some of their models, which is 40% higher than comparable modules based on lithium-ion technology.

Finally the GENeUSPACK [16] is able to sustain a voltage of up to 850 V of DC current and is also capable of storing up to 150 kWh.

## 2.7 Propeller

As it has already been mentioned, the plane's design includes a ducted fan as its source of aerodynamic efforts. However, since the program doesn't support any component or submodel representing that exact thrust generating model and for the simplicity of the simulation, a simple propeller that closely follow the parameters of the original ducted fan will be used.

Essentially, a ducted fan is a thrust-generating propeller inserted into a cylindrical duct or shroud. When compared to an isolated propeller of the same diameter and power loading, ducted propellers typically produce greater static thrust and since the actual fan is concealed and secured by the duct, it adds another layer of security which makes them specially advantageous when considering the integrity of unmanned or small/personal air vehicles [7].

These sorts of propellers are fundamentally defined by 3 parts.

- Fan: it is commonly known as rotor
- Duct: aerodynamic ring which surrounds and encloses the fan
- Powerplant: motor that supplies the necessary torque

In our project, the ducted fan which will be employed will feature a total of 5 blades with a NACA2412 2.45 shape following this pattern:

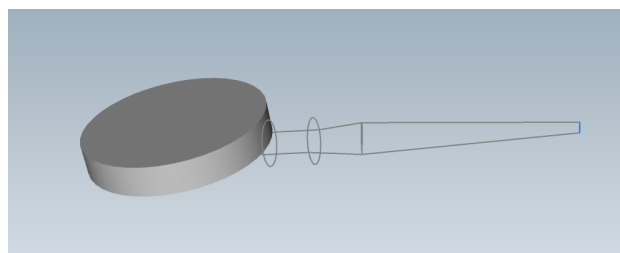


Figure 2.44 - Propeller of the ducted fan

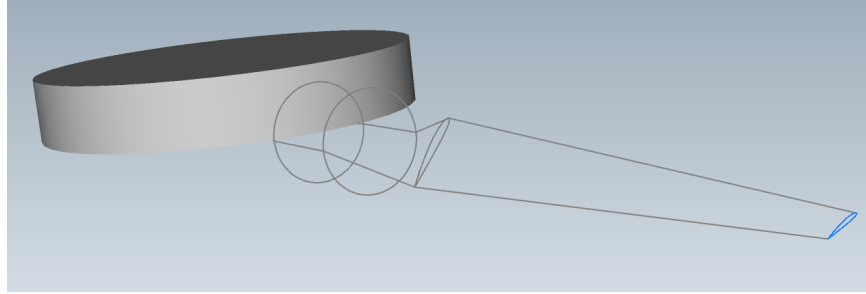


Figure 2.45 - *Profile of the blade*

Once inputted the geometric conditions the rotor, Amesim can generate tables 2.46 to look up crucial parameters such as the coefficients for thrust and power,  $C_t$  and  $C_p$  respectively.

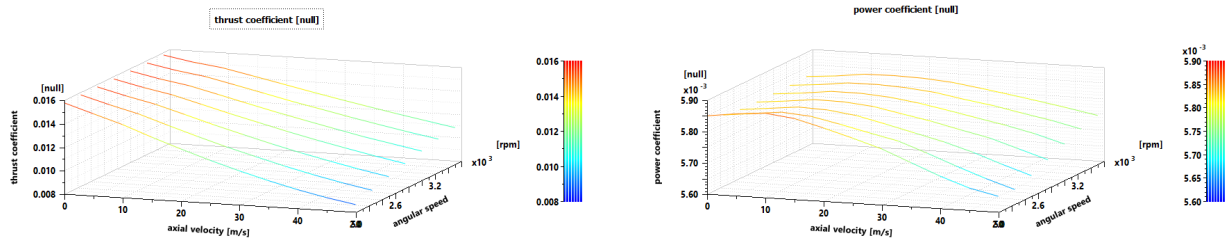


Figure 2.46 - *Maps of  $C_t$  and  $C_p$  for our rotor*

Thanks to these maps and a scaling tool that takes into account the pitch angle, the final result is this scaled map 2.47 with lets us choose the efficiency of the ducted fan as a function of the already mentioned angle. In our case, efficiency will be 74.95%,  $C_p$  will equal 0.0842 and  $C_t$  will equal 0.0387.

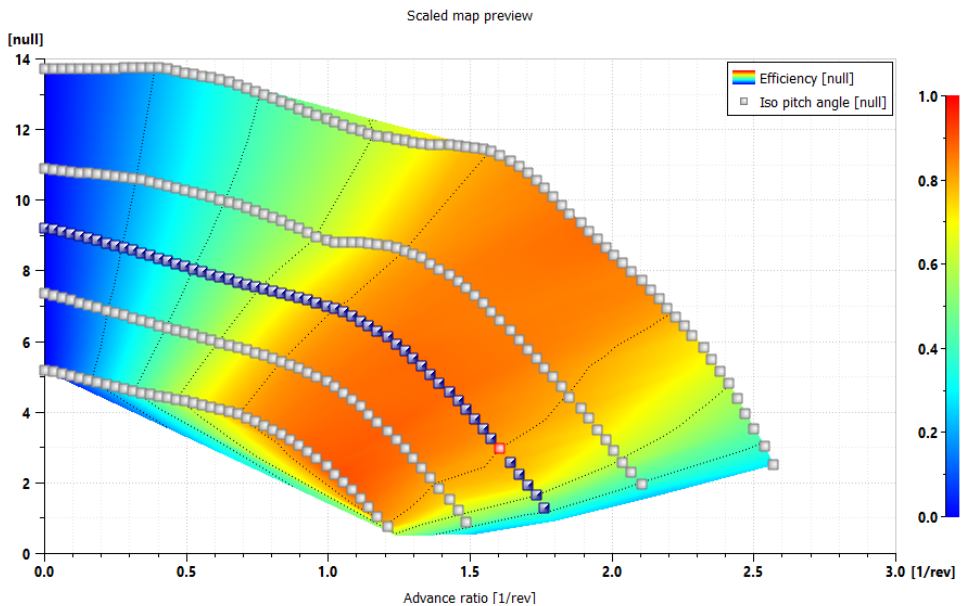


Figure 2.47 - *Efficiency map*

Finally, with all that data and the inputs that supply the component, the model calculates the quantities specified in 2.9. It does calculate the aerodynamic torque<sup>2.13</sup> as well:

$$\text{torque} = C_P \cdot \rho \cdot \pi \cdot \omega^2 \cdot R^5 \quad (2.13)$$

where

- $C_P$  is the coefficient of power,
- $\rho$  is the air density [ $\text{kg m}^{-3}$ ],
- $\omega$  is the angular velocity of the propeller [rev/s],
- $R$  is the radius of propeller [m].

## 2.8 TurboGenerator

Lets take a look at the inside of the already mentioned supercomponent used to encase the TurboGenerator model. As we can see in 2.48, it contains the usual components of a Brayton gas cycle .

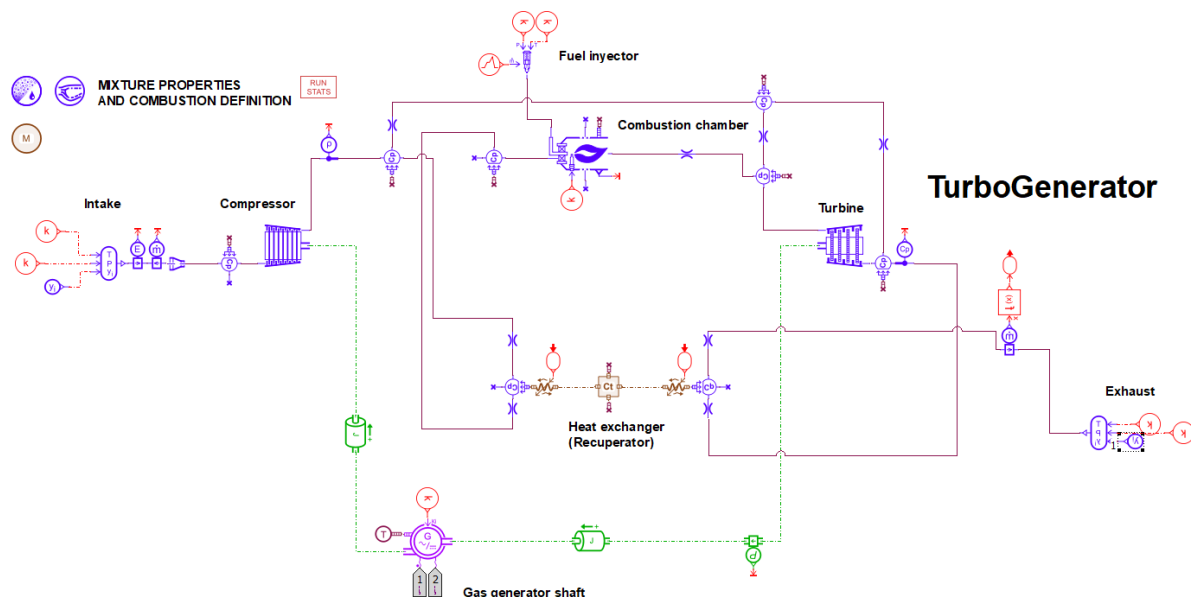


Figure 2.48 - *TurboGenerator Simulation*

In the last figure, we can see that the simulation accurately represents a Regenerative Gas Turbine cycle (RGT). At the top left corner, there are three components that define:

- Mixture of gases: it is possible to select the gases present in the air that will be employed in the combustion reaction. This is the one chosen:

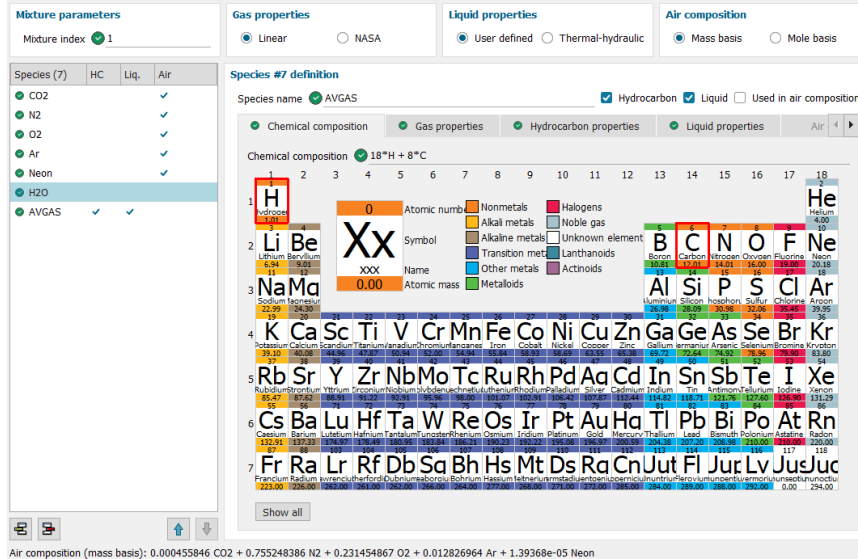


Figure 2.49 - Air Composition

- Combustion: to simplify the model, we will suppose that AVGAS 100 LL follows the usual empiric formula of gasoline and that the combustion is produced according to 2.14



- Material of the exchanger: according to [26], the tubes of the heat exchanger are made from Inconel, a austenitic nickel-chromium-based high temperature superalloys normally used in applications which require low expansion coefficients but even in this family, the exact composition remains undisclosed.

Besides, there is also a compressor, a turbine and a generator. Since there is practically no information on this components (TurboGenerator has not received EASA certification but it will receive it in 2025) from the real machine, a simple approach was the best way to simulate them. For the generator, it was simulated like the generator GENeUS 300 to keep this simulation from distancing too much from the couple Rotax 912 + GENeUS. For the compressor and turbine, they were modeled as single stage machines with a range of operation indicated by these graphs 2.50 2.48.

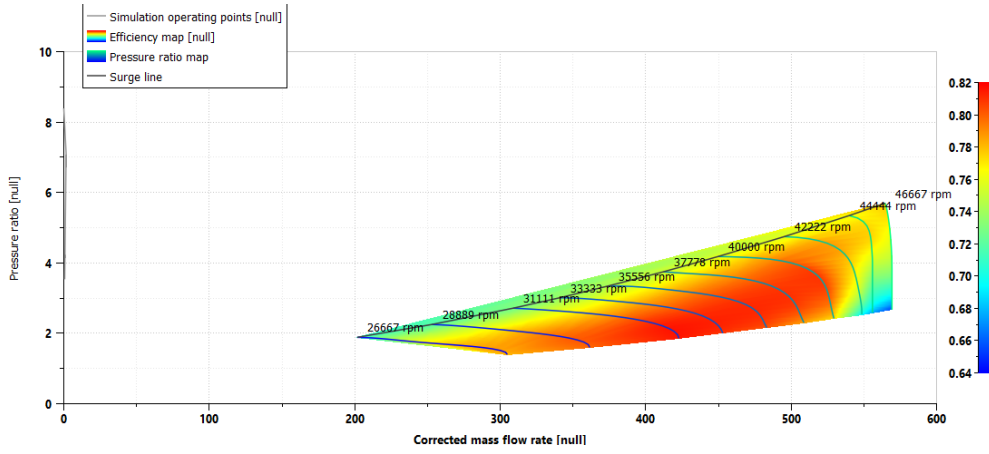


Figure 2.50 - *Compressor Map*

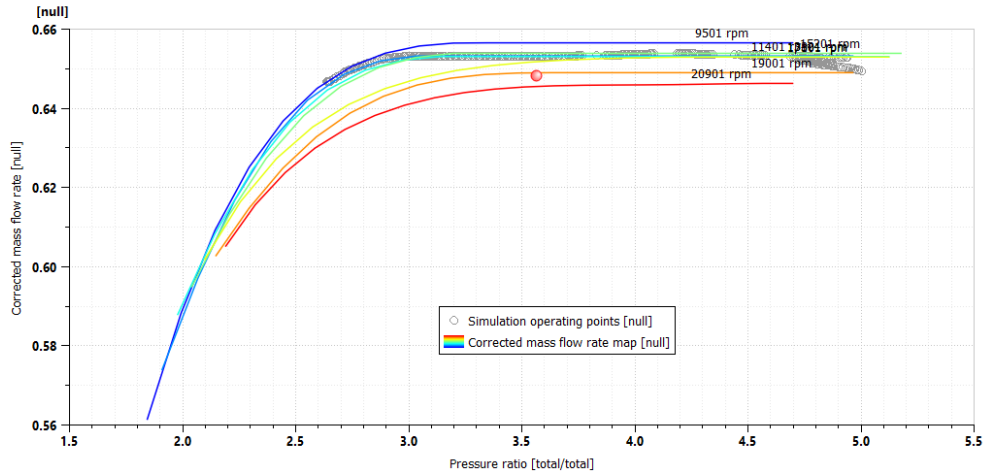
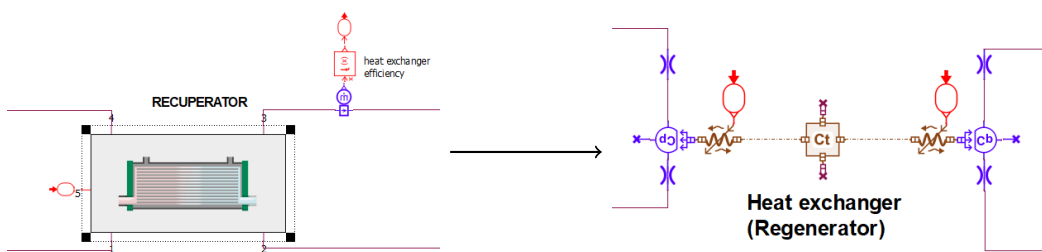


Figure 2.51 - *Turbine map*

For the recuperator, the modeling is very challenging since this is considered the most crucial part of the TurboGenerator and almost no data has been published about it. It was already mentioned that they have a patent on it and that, primarily thanks to it but also other design choices, the fuel efficiency of this machine can be increased from the expected 10% to the 26% - 30% assured by its creators [34]. Therefore, a recuperator from another similar simulation of a Brayton cycle will be employed.



# Chapter 3

## Simulation in AMESim

### 3.1 Characterising components and assumptions

It has already been explained the nature and the function of each part of the simulation. Besides, some of the components of the simulation are based on actual machines and products belonging to various enterprises portfolios. However, the way in which the information acquired has been adapted from the sources and the way that has been translated into parameters that the program can interpret hasn't been properly illustrated yet. This is topic for this section of the report.

#### 3.1.1 Mission Plan

By using the mission planner, a flight path was designed for our model. This flight plan is composed of a total of 9 phases which can be divided into 3 different types that essentially depend on the angle of attack of the plane:

- Climb
- Cruise
- Descent

The phases in which the flight plan has been based are the traditional ones followed by most recreational aircraft. It is imperative to remember that the Mindus VP is an aircraft designed and thought to act as a way for the public to experience a sightseeing flight and that its missions will not last more than 45 minutes in total.

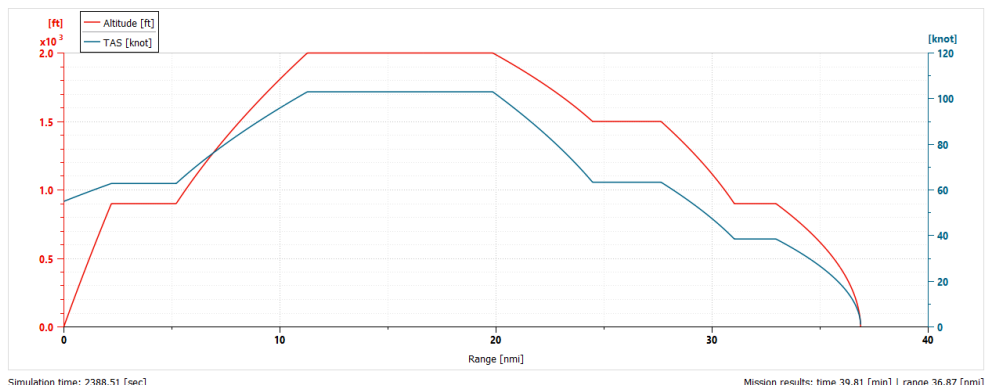


Figure 3.1 - *Flight Plan*

1. Take-off and initial climb: this is the phase in which the airplane ceases contact with the runway and it begins gaining altitude until it gets to a safe level. This phase lasts 2.24 minutes and the airplane reaches 900 ft.
2. Initial cruise: it is customary that small airplanes perform a loop around a predefined semi circuit close to the airfield to make and that is what's happening here. This phase lasts 2.87 minutes and the airplane covers a total of 3 nautical miles.
3. Main climb: once the semi circuit is completed, the aircraft starts climbing until it reaches the ideal or nominal altitude for which is designed. In our case, this climb lasts 4.4 minutes and the aircraft reaches 2000 ft.
4. Panoramic cruise: it is during this phase when both the pilot and the customer can enjoy the views from the high altitude point. In order to keep the expectations moderated, this phase will last for about 5 minutes although this quantity can surely be increased. The airplane will cover a distance of 8.58 nautical miles.
5. First descent: the plane decreases its altitude and begins heading for the airfield once again. This phase will last 3.33 minutes until a still impressive altitude of 1500 ft is reached.
6. Third cruise: the aircraft will continue its journey towards the airbase. This phase will last 3 minutes and the plane will cover 3.17 miles.
7. Second descent: it is in this phase when the pilot may begin communicating with the air control operators and air traffic controllers to explain their intentions and request permission to land. The plane will descent until it reaches 900 ft which will take about 4 minutes.
8. Approach: once the pilot has received confirmation, the plane will begin closing in on the airfield and redoing the semi circuit previously mentioned. This will be done during 3 minutes and a total distance of 1.93 miles will be covered.
9. Final approach and landing: the end of the journey happens when the pilot receives confirmation that the runway is empty and available. Then the plane will gradually descend towards the landing strip until it safely touches the ground. This phase is the longest one, by lasting a total of 11.97 minutes and covering a total of 4 miles.

In summary, this flight is designed to last almost 40 minutes without accounting for the taxiing at the beginning or at the end. A total of almost 37 nautical miles or 68 kilometers can be covered during one flight.

These values are the ones chosen to achieve pleasant and enjoyable experiences for customers, although they can be modified in terms of altitudes, speeds and times so that they better adapt to each customer's needs. Although, for the simulation, new equations would need to be inputted in the case of new flight phases.

### 3.1.2 Atmospheric conditions

Included in the simulation there is a submodel which accounts for the environmental impact that the plane has to deal with. This is another way to testify that the software's limits are extremely wide and that the complexity of the simulations can be pushed further and further depending on the ambition of the designer.

Title	Value	Unit	Tags	Name
environmental index	1			envindex
atmosphere model	ISA-76			atmmodel
gravity expression	constant			gravitymodel
earth representation	flat fixed earth			earthframe
define starting time	yes			userstarttime
gravity at Sea Level on equator	grav m/s/s			gravitysl
atmosphere				
delta ISA for temperature	0 degC			deltaISA
time				
starting year	2024			startyear
starting month	june			startmonth
starting day	24			startday
starting hour	9			starthour
starting minute	0			startminute
starting second	0			startsecond
time zone for defining starting time	0 null			timezone
daylight saving time	0			daysavingtime

Figure 3.2 - *Atmospheric Parameters*

This precise model will be based on the International Standard Atmosphere (ISA), which represents a static atmospheric model, published in 1976 by the International Civil Aviation Organization (ICAO), of how the pressure, temperature, density, and viscosity of the Earth's atmosphere change over a wide range of altitudes or elevations [9]. In 1993, the ICAO published the "ICAO Standard Atmosphere" as Doc 7488-CD, similar to the ISA of 1976 but extends the altitude coverage to 80 kilometers. There exists yet another atmospheric model, the US Standard Atmosphere, first published in 1958, but later updated in 1962, 1966 and 1976.

### 3.1.3 Control section

Although this section of the simulation has already been explained, there is a detail worth mentioning. This detail appears in the last equation of the control loop which is the one that, having as inputs the flight phase, the current angular speed of the shaft, power required by the shaft to comply with the mission demands, calculates the torque signal which will later be passed to the electric motor. Said equation, in the original model, is:

$$(z < 5) \cdot \frac{y}{x \cdot \frac{\pi}{30}} + (z \geq 5) \cdot \min \left( \frac{y}{x \cdot \frac{\pi}{30}}, \text{TmaxMOT} \cdot 0.25 \right) \quad (3.1)$$

While in my modified version, the equation is;

$$(z < 5) \cdot \frac{y}{x \cdot \frac{\pi}{30}} + (z \geq 5) \cdot \min \left( \frac{y}{x \cdot \frac{\pi}{30}}, \text{TmaxMOT} \cdot 0.7 \right) \quad (3.2)$$

where:

- z: is the flight phase
- y: represents the power required by the shaft [W]
- x: corresponds to the angular speed [rad/s]

- $T_{\text{MaxMOT}}$ : quantifies the maximum amount of torque that the ENGINeUS 100 can produce

The premise of this equation is that, when the program is calculating one of the 5 first flight phases, the first condition becomes true while the second is false and so, the output is the typical equation for torque. However, in case that the flight phase is the 5th or beyond, there is the possibility of a descent phase and there is where problems might arise. In order to avoid them, when the program calculates a descent phase, the second condition becomes true and the program has to identify the minimum value between the typical equation for torque and a percentage of the maximum torque of the motor. In our case, this corresponds to the 70% of the maximum power. The minimal quantity will be the signal sent to the motor.

All this conditions derive from the fact that the program can not sustain very well negative angles of attack and it makes a small error when calculations are ran. This mistake gets amplified with each calculations because of the feedback loop nature of this section, leading to amount of power and torque required by the shaft to spiral out of control 3.3. Due to this the simulation crashes because the software cannot work with such high values.

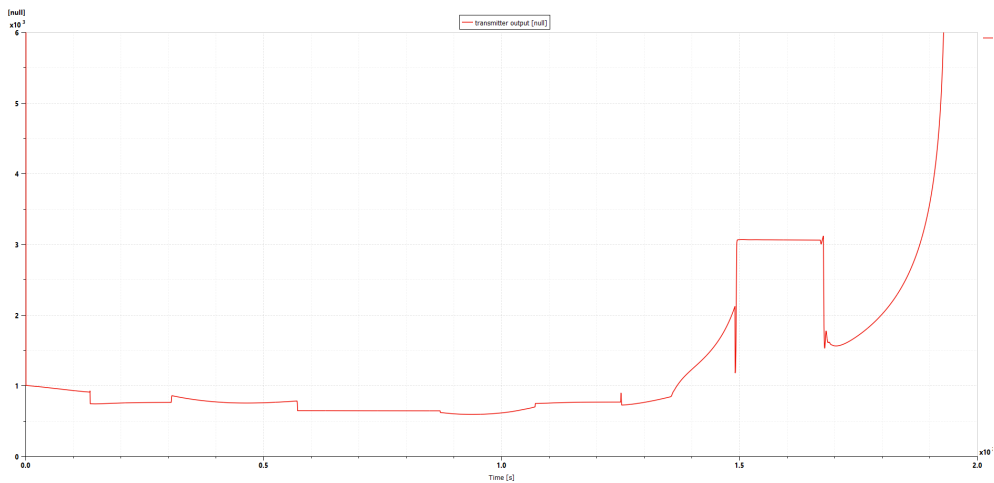


Figure 3.3 - *Power required without the correcting factor*

### 3.1.4 Engine Characterisation

There is various ways of modelling an internal combustion engine in Simcenter Amesim such as the IFP-Engine library, the IFP-Drive library or detailed models. The last option is completely discarded as those previously mentioned models are extremely complicated 3.4 to the point that it would be impossible to get all the information needed to support them from Rotax, thus making the models inaccurate and ultimately useless. Also, even if the IFP-Engine library offers components with moderate a degree complexity and fidelity, they are hardly able to communicate with components that dictate other data such as signals, paths etc.

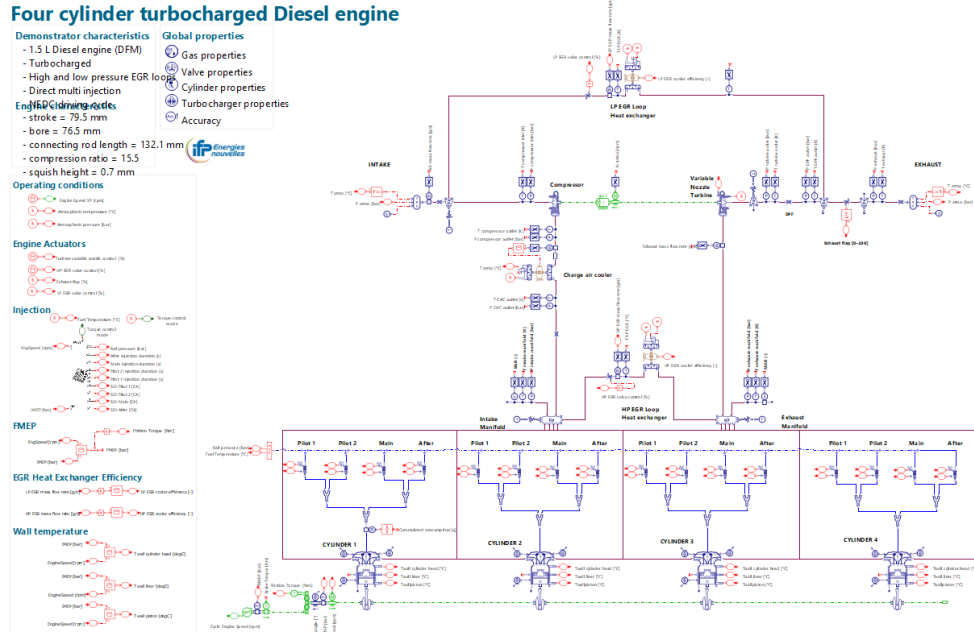


Figure 3.4 - Fully working model of a Diesel Combustion Engine

Therefore, to model the Rotax, employing the IFP-Drive library which already contains a model that can be tuned with the usage of the tables and other parameters, seems the best alternative.

For starters, the ECU has to receive a signal displaying what is the actual combustion mode since the program allows for different combustion modes which means it can operate between different tables of performance. In our case, there is only one combustion mode so the signal will be constant. Besides, the ECU communicates a signal for the demand of power. The ECU allows for different options of demand signal such as torque, powertrain power or even a signal between 0 and 1. In our case, a signal was designed on table 3.5 which takes into account the time duration of each phase of the mission and each amount of power needed.

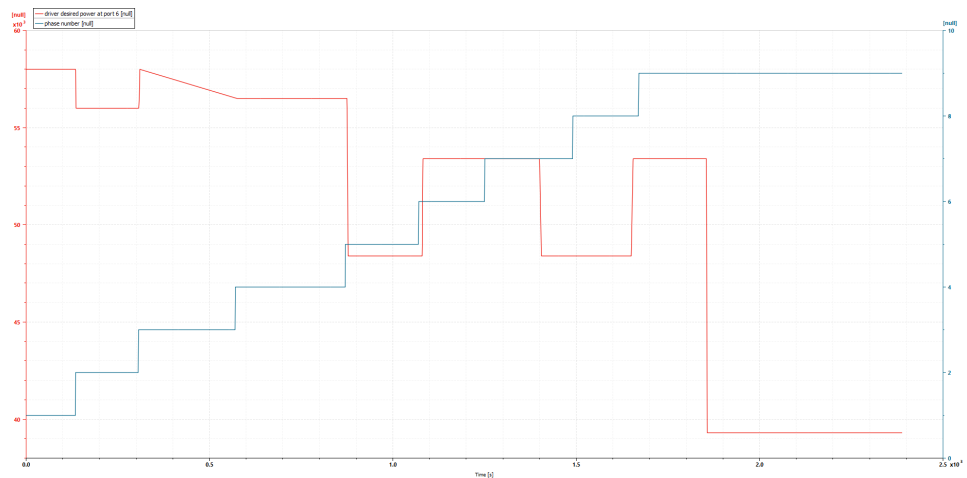


Figure 3.5 - Power demand signal and the according flight phases

After preparing the signals that will be transmitted into the ICE via the ECU, next step was to correctly characterise the way that the Rotax 912 works. The submodel has a tool that, given a series of parameters regarding geometry, type, fuel characteristics and applications, can generate its own maps for the performance of the engine. However, after performing some experimental trials, this tables dont seem to be accurate at all so instead, personally designed tables 3.6 will be used, based on my calculations for which values from [21] were taken. This is the result:

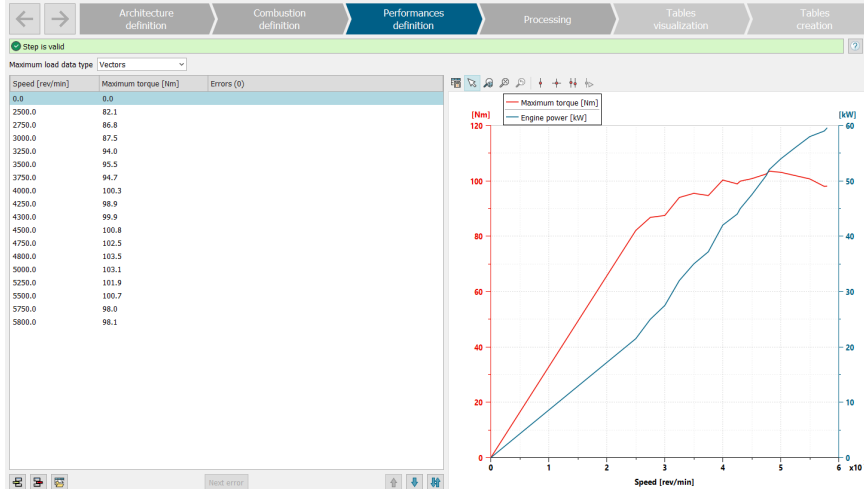


Figure 3.6 - Performance of the engine

Apart from this, other quantities needed to be defined such as the number of pistons, the bore measures, the displacement, the units of the tables inputted into the software and even the results that we expect form the mode. In our case, interesting result will be:

- Torque produced
- Fuel consumption
- Exhaust emissions

In order to give enough information to the software for the calculation of emissions, series of tables were created, again from my own calculations, for each specie of major pollutant that the engine can track. These are CO<sub>2</sub>, CO, NO and scoot matter, and all the data was taken from [27]. This are the results:

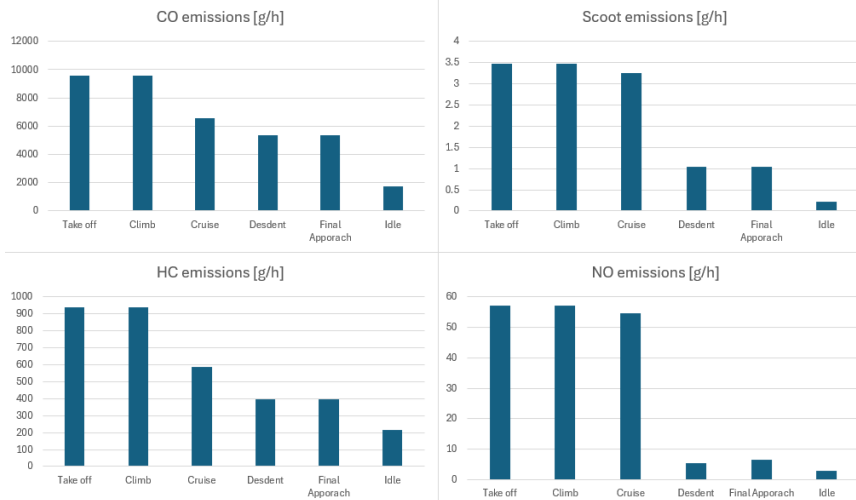


Figure 3.7 - *Calculated values for the grams of pollutants per hour*

Precise and definitive results on the flow and the amount of pollutants will be displayed in the following chapter.

### 3.1.5 Generator and Motor Characterisation

As most components of this simulation, the electrical models which have been based on the products of Safran could have been modelled with greater or fewer detail. However, doing this is quite difficult because of mainly 2 reasons:

1. Due to the extremely innovative technologies used for these designs, the actual limitations and some of the specifications have to remain private and undisclosed. Also, since the products are quite new, new models of the belonging to the same families are being continuously developed.
2. There are few studies, articles, reports and technical documentation online and available which makes the gathering of data quite more difficult.

Therefore, the option of parametrising the models in a simple way was selected, without the use of advanced and detailed tables or expressions.

For the generator:

- Minimum speed for generator to deliver current: 1500 rpm
- Minimum speed for generator to deliver maximum current: 5500 rpm
- Maximum generator current: 215 A
- Constant efficiency: 96%
- Maximum power generated: 300 kW

For the electric motor:

- Constant efficiency: 95%

- Maximum power generated 180 kW
- Maximum angular speed: 3500 rpm
- Continuous angular speed: 2750 rpm
- Power density: 5 kW/kg
- Mass: 36 kg

### 3.1.6 Battery

Even though the battery is based on the Sagran's ENGINeUSPACK, this product is the most secretive since only the maximum energy capacity has been published, which is around 150 kWh. Therefore, my own calculations will be used and the methodology and equations displayed in [35] will be employed.

Firstly, this is the listing of the data that we have and will be using to calculate the proper values for the correct battery sizing, following the steps of the preciously mentioned master thesis.

- Weight of the plane -  $W = 530 \text{ kg}$
- Energy weight fraction -  $\beta = 0.4$

This parameter accounts for the amount of mass of the airplane that is destined for an energy source which is the battery or the gas

- Charging fuel weight fraction -  $\alpha = 0.5$

This parameter quantifies the amount of fuel destined to generate electricity to charge the battery

- Lift-to-Drag ratio -  $L/D = 5.5$
- Endurance -  $t = 1 \text{ h}$
- Motor Voltage -  $V_{motor} = 800 \text{ V}$
- Cell capacitance -  $Q_{cell} = 3.3 \text{ Ah}$
- Nominal Cell Voltage -  $V_{cell} = 4 \text{ V}$
- Minimum Cell Voltage -  $V_{min} = 3 \text{ V}$
- C-rate discharge -  $C_{dis} = 1 \text{ C}$
- Cell battery weight -  $W_{cell} = 45 \text{ g}$
- Battery Knockdown value -  $W_c = 1$

This parameter accounts for the electronics and other various parts of the battery that add weight. We will assume it has no impact since the ENGINeUSPACK features an all-in-class smart desgin.

Also, we will impose similar constrains as the study did:

1. Range must reach at least 100 nm

2. In case of emergency, the battery must be sized to deliver 50 HP for 5 minutes to be able to safely land

Furthermore, we need to take into account the various crucial efficiencies for our model since it isn't ideal. Also, the composed efficiencies will be listed.

- Efficiency of the ICE -  $\eta_{eng} = 0.3$
- Efficiency of the generator -  $\eta_{gen} = 0.96$
- Efficiency of the power electronics -  $\eta_{PE} = 0.95$
- Efficiency of the battery -  $\eta_{bat} = 0.9$
- Efficiency of the electric motor -  $\eta_{EM} = 0.95$
- Efficiency of the propeller -  $\eta_{prop} = 0.7495$
- Efficiency from the fuel to the propeller -  $\eta_{f-prop} = 0.1948$
- Efficiency from the battery to the propeller -  $\eta_{bat-prop} = 0.6088$
- Efficiency from fuel to battery -  $\eta_{charg} = 0.288$

Lastly, the only values we are missing are the energy densities from both energy sources: AVGAS 100 LL fuel and the cell from the ENGINeUSPACK. Data from [10] and [15]

- Energy density of AVGAS 100 LL -  $\rho_g = 44 \text{ MJ/kg}$
- Energy density of the cells -  $\rho_b = 0.28 \text{ kWh/kg}$

Secondly, we will use 3.3 in which we will impose the first constrain that determines the minimal range of 100 nm:

$$x_{max} = \frac{Rg - \frac{L}{D}\beta * (\eta_{bat-prop}\eta_{charg}\rho_g\alpha + (1 - \alpha)\eta_{f-prop}\rho_g)}{\frac{L}{D}\beta * (\eta_{bat-prop} * (\rho_b - \eta_{charg}\rho_g\alpha) - (1 - \alpha) * \eta_{f-prop}\rho_g)} \quad (3.3)$$

where:

- R is the range [m]
- g is the acceleration of gravity [m/s<sup>2</sup>]
- $\rho_g$  and  $\rho_b$  are the energy densities of the gas and the cells respectively [m<sup>2</sup>/s<sup>2</sup>]

The result is that, as a maximum allowable percent hybrid x= 97.19%. Beyond this, the aircraft would not be able to reach the 100 nm range. We must recall that maximum range occurs when percent hybrid is minimized.

Next step is to use the equations 3.4 and 3.5 to find the number of cells of the battery. Some of the values such as the  $V_{cell}$  or the  $V_{min}$  have been estimated and can be modified for other uses. In addition, the emergency power we have selected can be tuned as well.

$$N_s = \frac{V_{motor}}{V_{cell}} \quad (3.4)$$

$$N_p = \frac{P_{emer}}{V_{min}\eta_{EM}N_sQ_{cell}C_{dis}} \quad (3.5)$$

where

- $P_{emer}$  is the emergency power we opted for [W]

The result is a total of 200 cells in series and 20 cells in parallel, We will use this data to calculate the total weight of the battery via equation 3.6.

$$W_{bat} = \frac{N_s N_p W_{cell}}{W_c} \quad (3.6)$$

This results in the battery weighting  $W_{bat} = 178.4$  kg, which represents around 33% of the total maximum take off weight of the plane. This is the perfect example to show one of the main and most difficult problems to solve with electric and hybrid aviation. In order for the batteries to suffice and fulfilled the current demands for the public, they must be designed extremely carefully so that their weight does not become an obstacle for the aerodynamic performance.

Finally, lets calculate with equation 3.7 the minimal percentage of hybrid required for the plane to comply with the constrain number 2.

$$x_{min} = \frac{W_{bat}}{\beta W} \quad (3.7)$$

The result is that  $x_{min} = 84.15\%$ . Therefore these are the results

Table 3.1 - *Constraints of the hybrid design*

#	Constraint	Percent Hybrid Limit
1	Range $> 100$ nm <sup>2</sup>	$x < 97.19$
2	Emergency 50 HP for 5 minutes	$x > 84.15$

Now lets consider that we change some of the expectations from our design, which can lead us to some interesting results:

- If choose to employ a less powerful electric motor which instead of working at 800 V works at 400 V, the number of cells for the battery would change although the weight will remain the same. Concretely,  $N_s = 100$  and  $N_p = 40$ .
- If cell technology advances much more rapidly and it is possible to develop a cells whose minimum voltage reaches  $V_{min} = 18$  V, that is 6 times more than it is now, the results are surprising. The number of cells in parallel  $N_p = 3$  but the battery weight  $W_{bat} = 29.7$  kg and the  $x_{min} = 14\%$
- Lets say that, instead of relying on the advancement of technology, we lower the emergency power to  $P_{emer} = 20$  HP. This will mean that the battery will have his weight more than cut in half with an impressive  $W_{bat} = 71$  kg and the  $x_{min} = 33.66\%$
- Also, if any improvements are done in parameter such as the efficiencies,  $\eta_{eng}$  for examples is the lowest and thus the more easily optimizable, or energy densities, the operational prices would go down significantly.

### 3.1.7 Aerodynamics and weight

In the description of the simulation section of Chapter 2, two components were mentioned and described : the aircraft submodel and the aerodynamics submodel.

For the first one, some already known values, taken from [29], were specified like the maximum take off mass, the measurements of the landing gear and its mass, the wingspan and the wing area etc. Furthermore, this subsystem can account for the mass loss of the plane while it travels which logically indicates that the mass loss due to fuel consumption can be computed into the system. However, in the original simulation, the weight was left as a constant and this feature wasn't used.

In order to be able to use it, firstly measurements were taken from [21], which included the already shown consumption graph 2.37. With those measurements, a M1D consumption table was programmed 3.8 from which it is possible to extract the value of fuel consumption based on the angular speed of the Rotax 912 and the Break Mean Effective Pressure (BMEP).

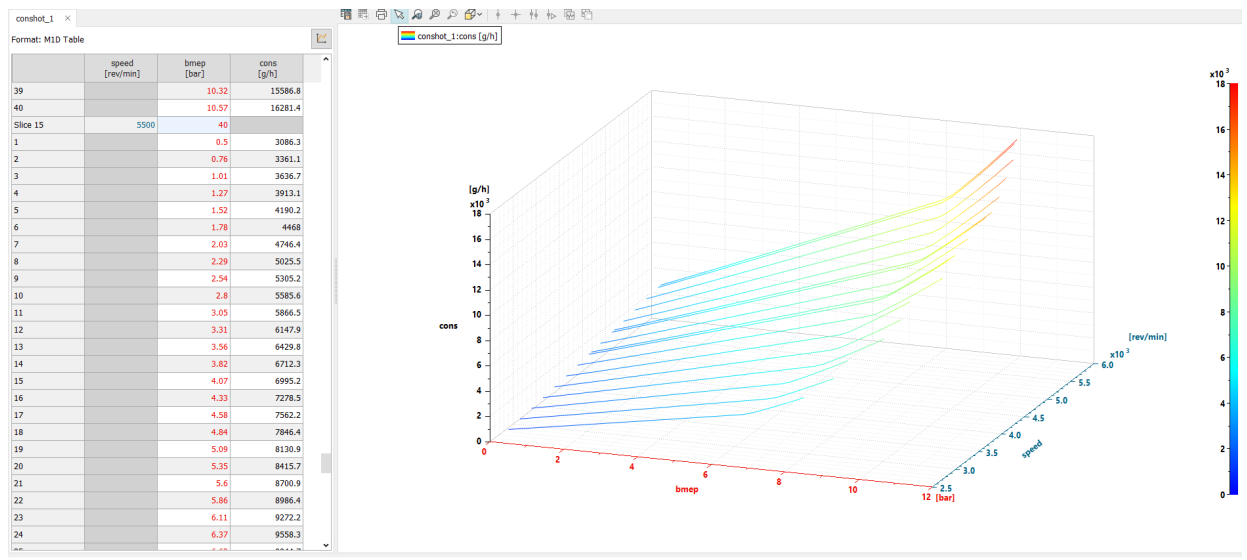


Figure 3.8 - Multiple 1D table of fuel consumption

Once this table was arranged, a small system 3.9 which automatically calculates the consumption of the plane based on the last table, was devised. The concept is that, based on the number of revolutions per minute of the shaft that exits the Rotax 912, the first M1D look up component gets the value of the Break Mean Effective Pressure of the engine at that moment. Knowing this parameter, the signal is communicated to yet another M1D look up component which, using again the signal from the angular velocity of the engine's shaft, calculates the fuel consumption by using 3.8. The only inconvenience is that the units for the value for the consumption is in g/h. Therefore, by following this equation 3.8, we get that the conversion factor is  $-2.7778 \times 10^{-7}$  and thus, we get the consumption in the proper units

$$kg/s = g/h * \frac{1kg}{1000g} * \frac{1h}{3600s} \quad (3.8)$$

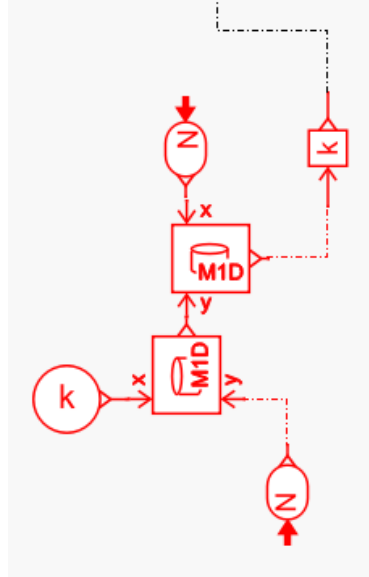


Figure 3.9 - *Weight loss by consumption*

For the second component, the aerodynamics equation component, the equations for the coefficients of drag and lift were needed. Firstly, we needed a table which, including the values for the  $C_{L0}$  and  $C_{L\alpha}$  taken from [29], calculates the  $C_L$  based on 3.9.

$$C_L = C_{L0} + C_{L\alpha} \alpha \quad (3.9)$$

where:

- $C_{L0}$ : Coefficient of lift at zero angle of attack,
- $C_{L\alpha}$ : is the Lift curve slope,
- $\alpha$  : is the Angle of attack (in radians)

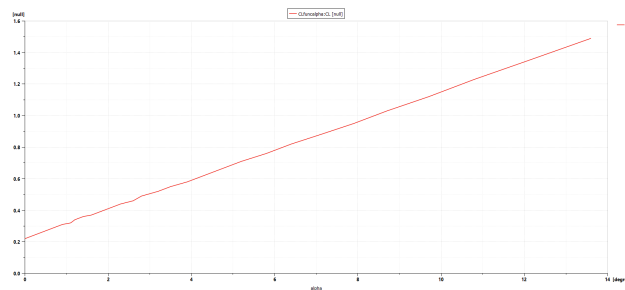


Figure 3.10 - *Coefficient of lift as a function of angle of attack*

Next step was to define the equation for the coefficients of drag, that is the other missing piece of the simulation. Continued by imposing the equation 3.10 for the 2D coefficient of drag.

$$C_{D2d} = C_{D0} + kC_L^2 \quad (3.10)$$

where:

- $C_{D_0}$  : Zero-lift drag coefficient
- $k$  : Constant related to induced drag
- $C_L$  : Coefficient of lift

After, the equation 3.11 was used to calculate the 3D coefficient of drag. This one accounts for the the aspect ratio and the induced drag.

$$C_{D3d} = C_{D0} + \frac{C_L^2}{\pi e AR} \quad (3.11)$$

where:

- $C_{D3d}$  : 3D coefficient of drag
- $e$  : Oswald efficiency factor
- $AR$  : Aspect ratio

All the data was taken from [29], in which the values were spread into the different sections regarding the different flight phases. Data for the descent phases was taken form the "Best Endurance" section. These are the final equations 3.11 for the drag coefficient.

table or expression for drag coefficient		
filename or expression for CD [null] = f((CL=null) or ...	<b>0.0228+(CL**2/(3.1416*1.14*0.835))</b>	CDFileExp1
filename or expression for CD [null] = f((CL=null) or ...	<b>0.02012+(CL**2/(3.1416*0.837*1.14))</b>	CDFileExp2
filename or expression for CD [null] = f((CL=null) or ...	<b>0.0228+(CL**2/(3.1416*1.14*0.835))</b>	CDFileExp3
filename or expression for CD [null] = f((CL=null) or ...	<b>0.02012+(CL**2/(3.1416*0.837*1.14))</b>	CDFileExp4
filename or expression for CD [null] = f((CL=null) or ...	<b>0.02356+(CL**2/(3.1416*0.835*1.14))</b>	CDFileExp5
filename or expression for CD [null] = f((CL=null) or ...	<b>0.02012+(CL**2/(3.1416*0.837*1.14))</b>	CDFileExp6
filename or expression for CD [null] = f((CL=null) or ...	<b>0.02356+(CL**2/(3.1416*0.835*1.14))</b>	CDFileExp7
filename or expression for CD [null] = f((CL=null) or ...	<b>0.02012+(CL**2/(3.1416*0.837*1.14))</b>	CDFileExp8
filename or expression for CD [null] = f((CL=null) or ...	<b>0.02356+(CL**2/(3.1416*0.835*1.14))</b>	CDFileExp9
discontinuity handling for CD table	active	discCD
linear data out of range mode for CD	extreme value	lmodeCD

Figure 3.11 - Final equations for  $C_d$

# Chapter 4

## Results and discussion

In this chapter, some of the results that the simulation has provided will be presented. It is paramount to emphasize that AMESim is a very wide range program in terms of applications and, even though a limited number of graphs will be showed, this software allows for the possibility of mapping and studying with various degrees of detail almost any quantity present in the current developed model.

The run parameters are set following the next values:

- Simulated time: 2388.11 seconds
- Number of points: 4777
- Sampling frequency : 1.999 Hz
- Saved variables: 711
- Estimated size: 26 MB
- Estimated size (TurboGenerator): 55 MB
- Tolerance:  $1 \times 10^{-7}$

It is important to warn that most of these results will be taken from the simulation that features the generating couple of the ICE Rotax 912 UL and the generator GENeUS 300. Some results that don't depend on the generation method will remain the same. However, for the ones that are directly related to the TurboGenerator itself or are influenced by the simulation that contains it, these will be marked and properly explained.

### 4.1 Plots and graphs

First of all, the paramount result of this simulation is whether the Mindus VP can achieve the mission and return back to safety while employing all the different machines and structures which have been mentioned in this report.

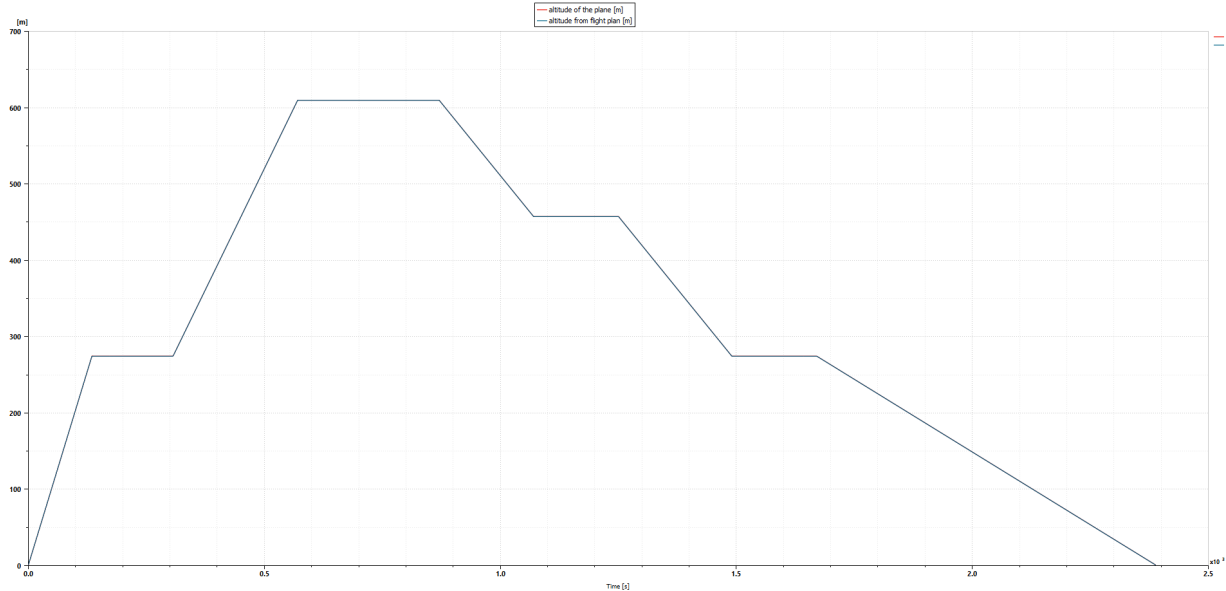


Figure 4.1 - *Flight Mission vs Actual Flight*

In the graph 4.1, we see two lines which completely overlap. These are the designed flight path and the altitude of the center of mass in the plane and as we can see the plane managed to follow what was established with impressive accuracy. In fact, during the whole flight, the difference between the both paths is around 0.1 m. That means an error that is of around 0.03% if we consider an average altitude of 300 m.

Also, lets look at the forces experience by the aircraft.

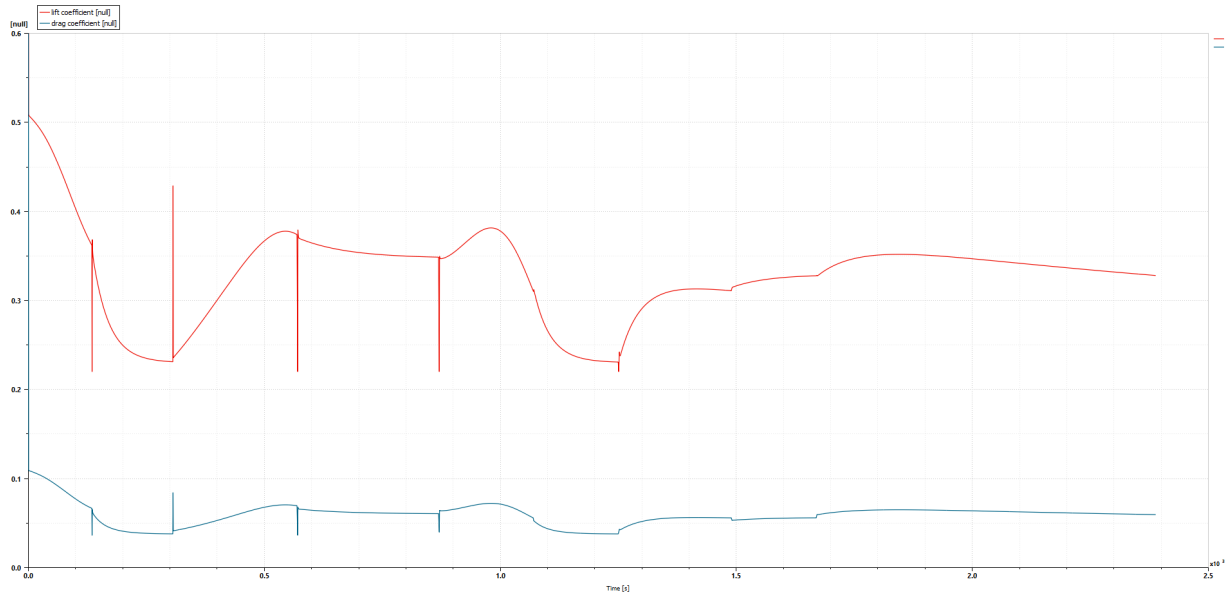


Figure 4.2 - *Coefficients*

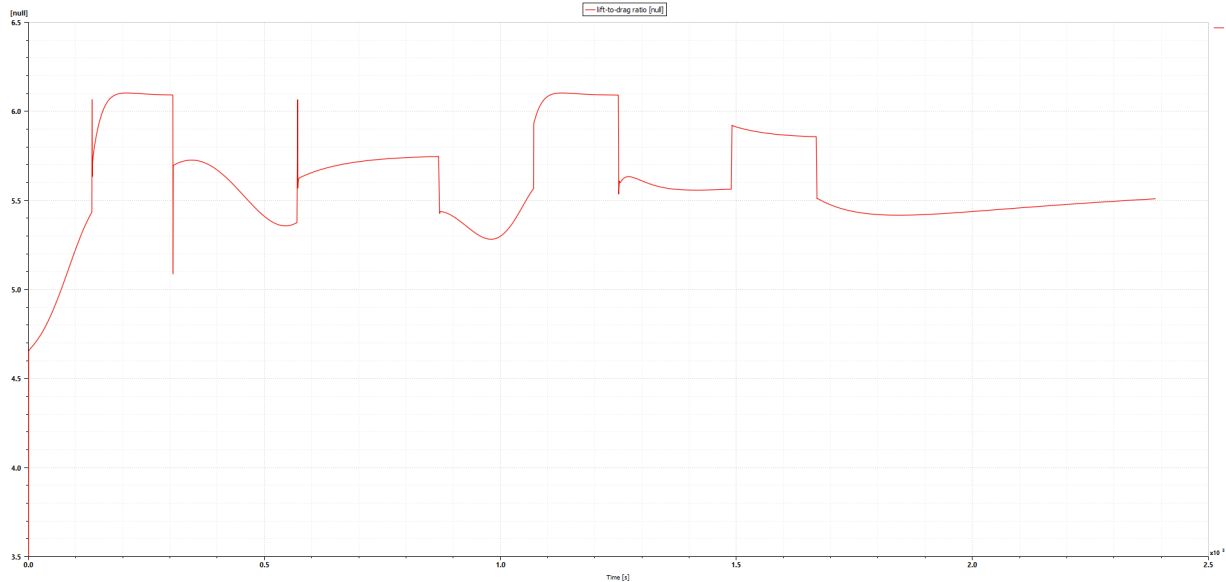


Figure 4.3 - Lift-to-drag ratio

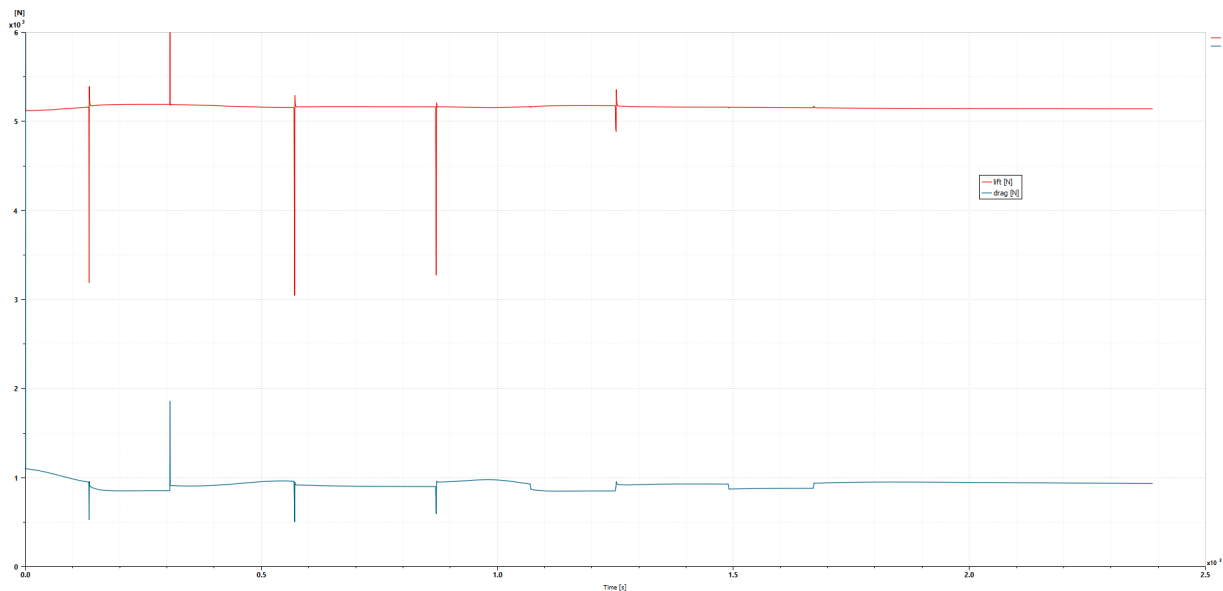


Figure 4.4 - Lift vs Drag

It is easy to appreciate that the values of the coefficients 4.2 4.3 change depending on the flight phase since the angles of attack. It is also notable that there are spikes at the end of each flight phase, which can be attributed to harsh changes in the parameters used for the calculations. Besides, the values for lift and drag remain quite predictable, with the first oscillating around 5100 N while the latter oscillates around 1000 N.

Now lets check the propulsion power 4.5 outputted bu the ducted fan.

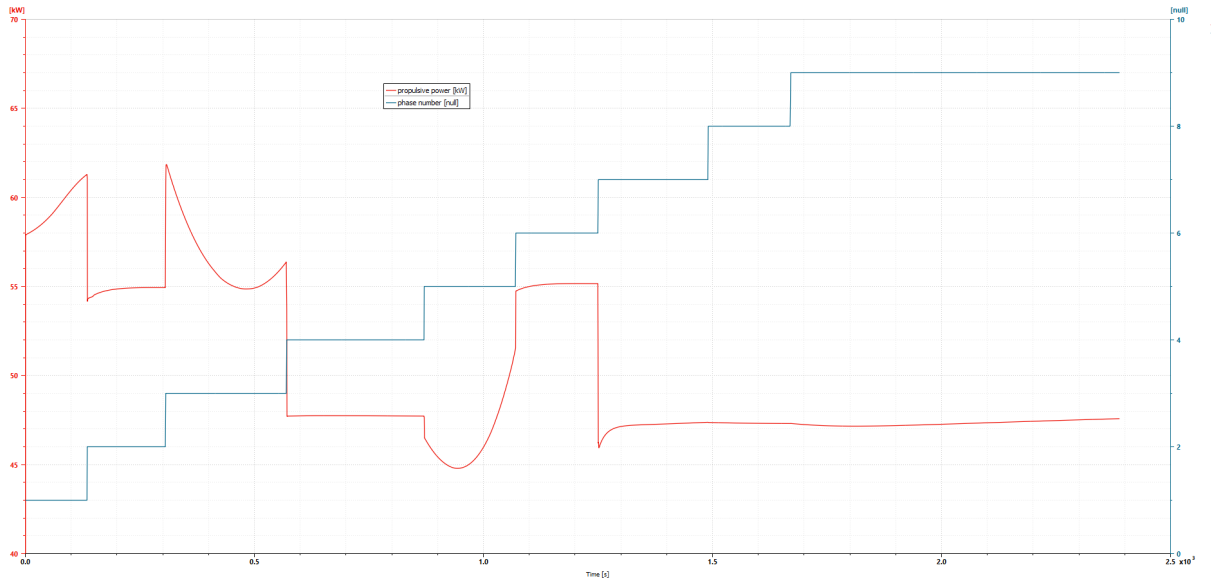


Figure 4.5 - Propulsive power coming from the fan in reaction with each flight phase

It is noticeable that during the climbing phases, the propeller needs to exert more power to keep the plane ascending while in the cruise phase, it remains constant. Also when the condition imposed in the torque equation takes charge of the signal sent to the electrical engine, this can be seen as a constant power output. This shape 4.6 can also be reflected in the torque provided from the ENGINeUS.

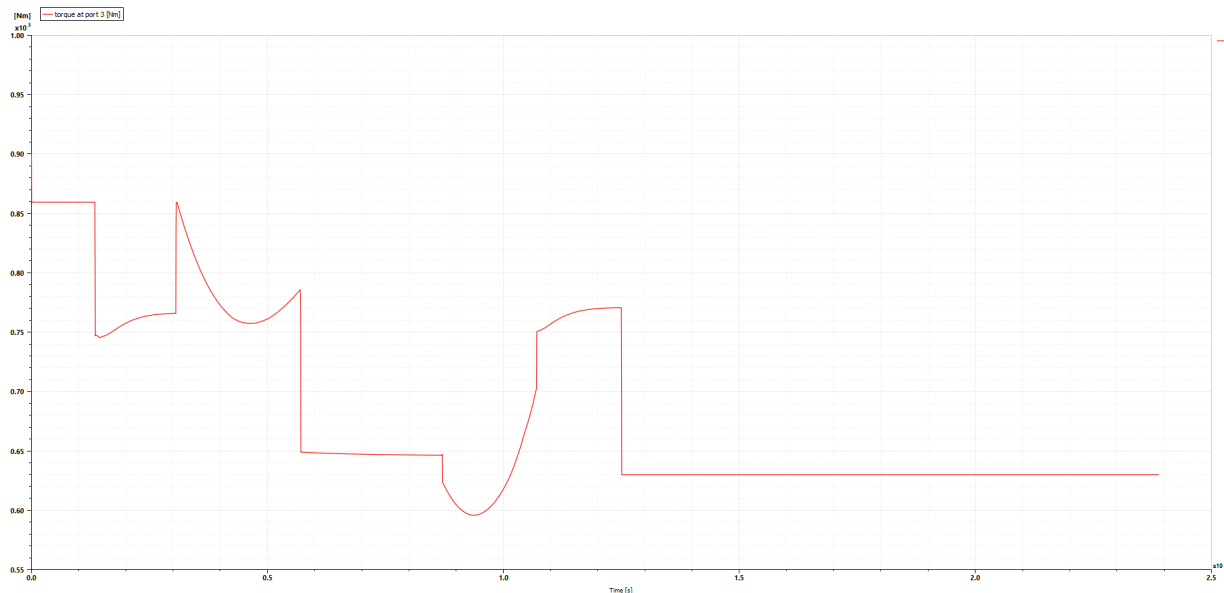


Figure 4.6 - Torque signal provided by the electric motor

Furthermore, let's see how the generating couple of components have worked.

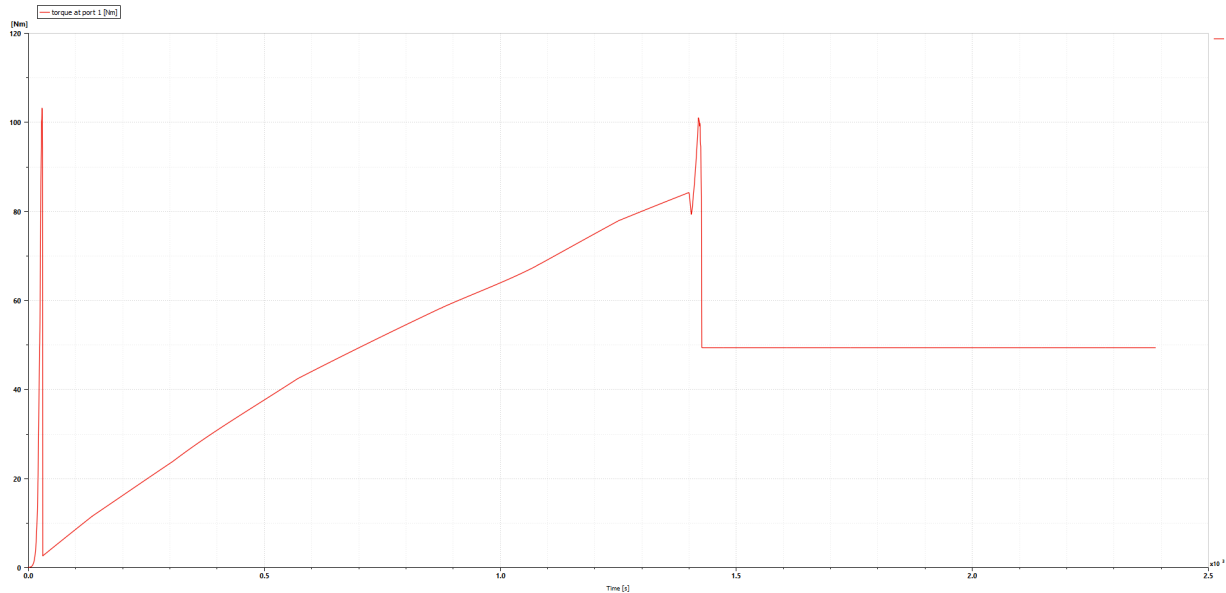


Figure 4.7 - *Torque signal provided by Rotax 912 UL*

The graph 4.8 shows how the torque transmitted by the engine to the generator evolves during the mission time, until it stabilizes for the descending phases. Also, in 4.9, we see how the ICE efficiency changes through time.

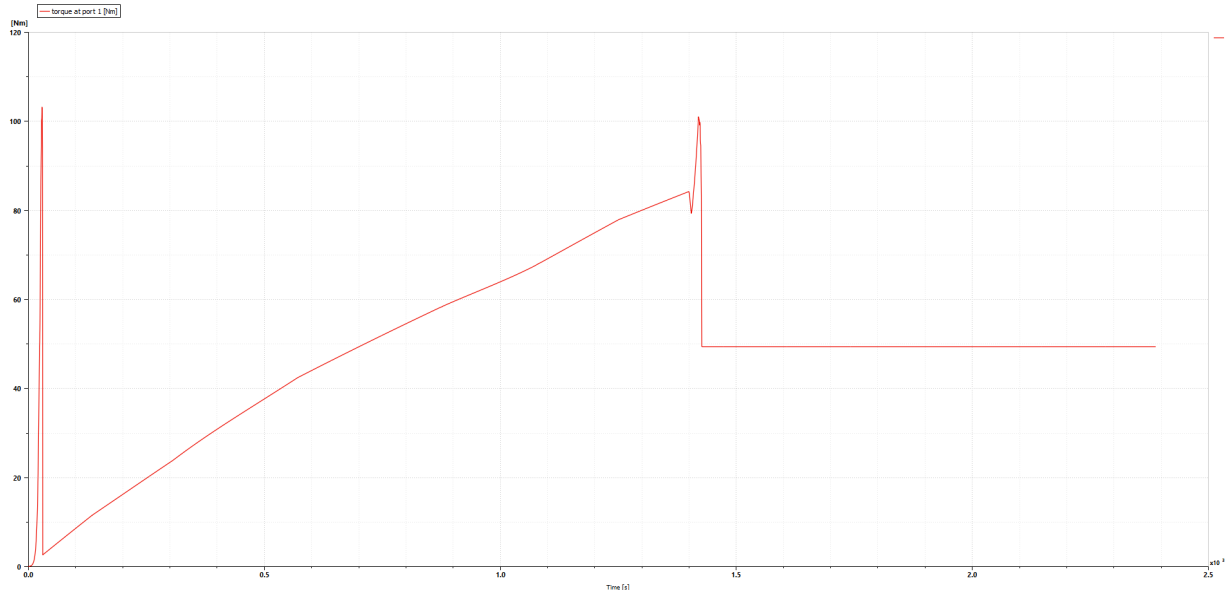


Figure 4.8 - *Torque signal provided by Rotax 912 UL*

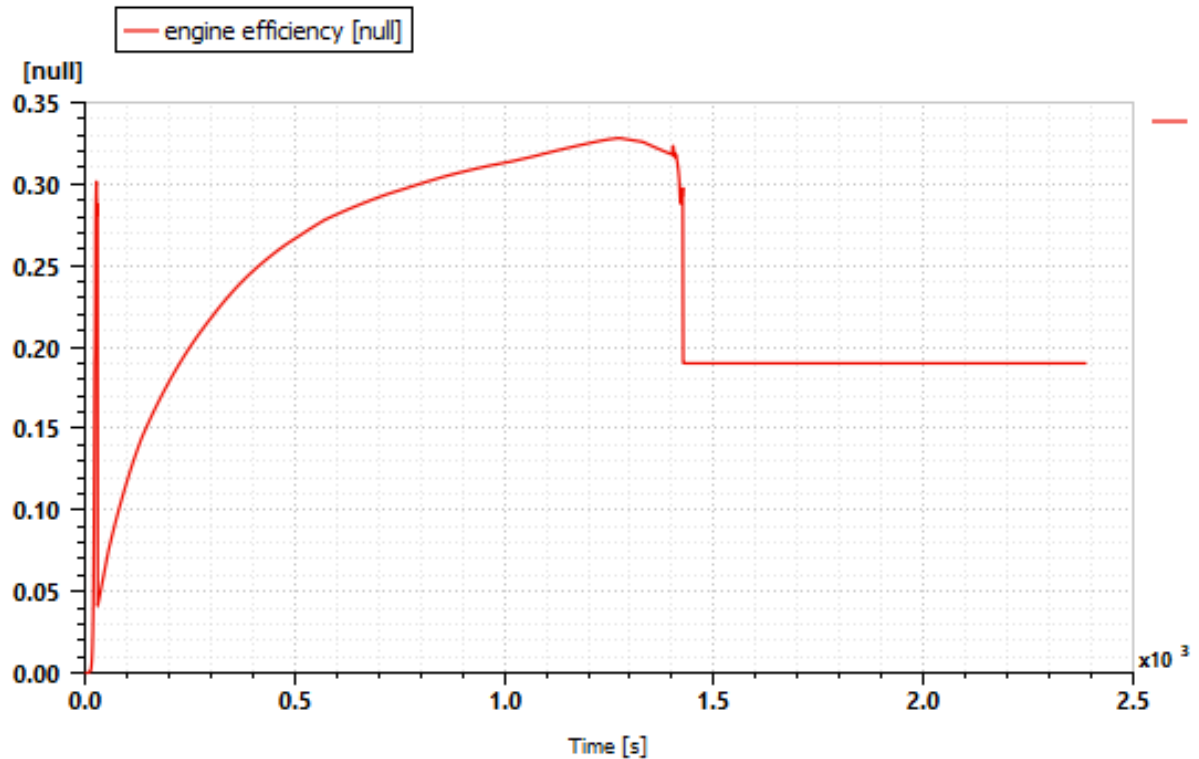


Figure 4.9 - *Engine efficiency of the Rotax 912 UL*

On the other hand, the electrical power produced by the generator 4.10 reminds us of the familiar shape that we have already seen in other graphs.

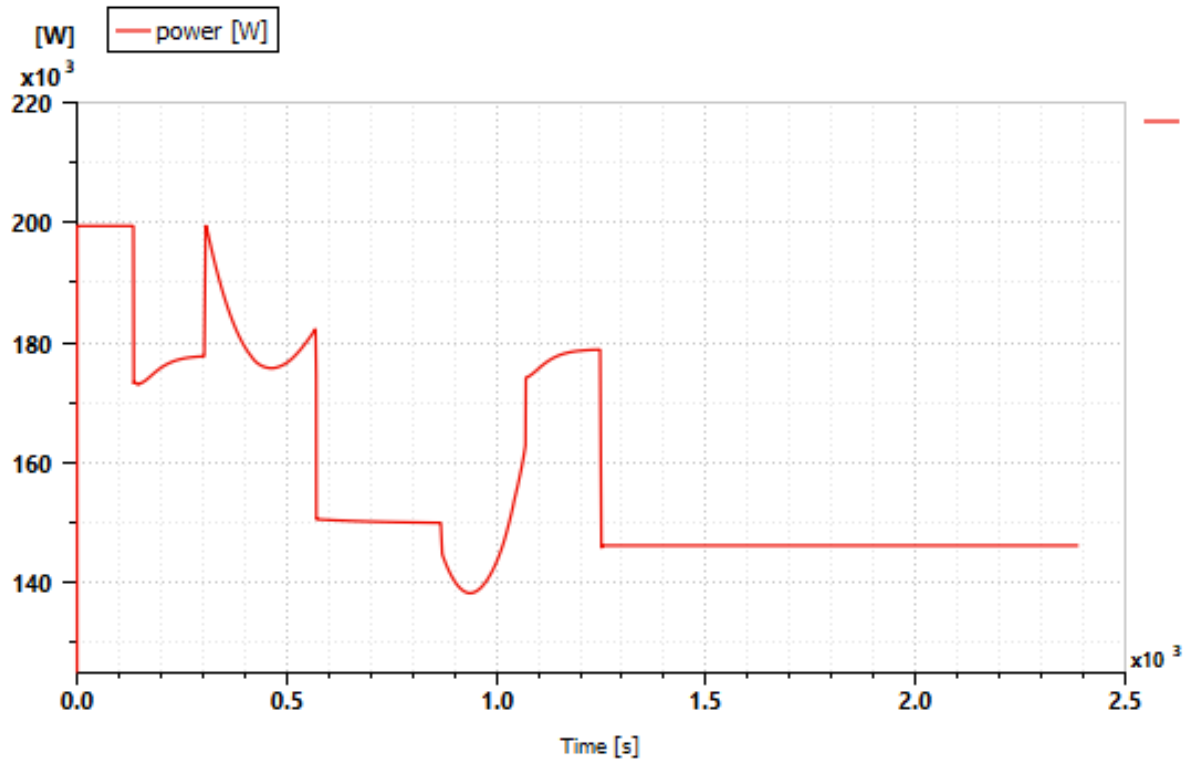


Figure 4.10 - *Electrical power from the GENEUS 300*

Additionally, lets see how the battery has depleted during the time that it has been providing power to the aircraft motor.

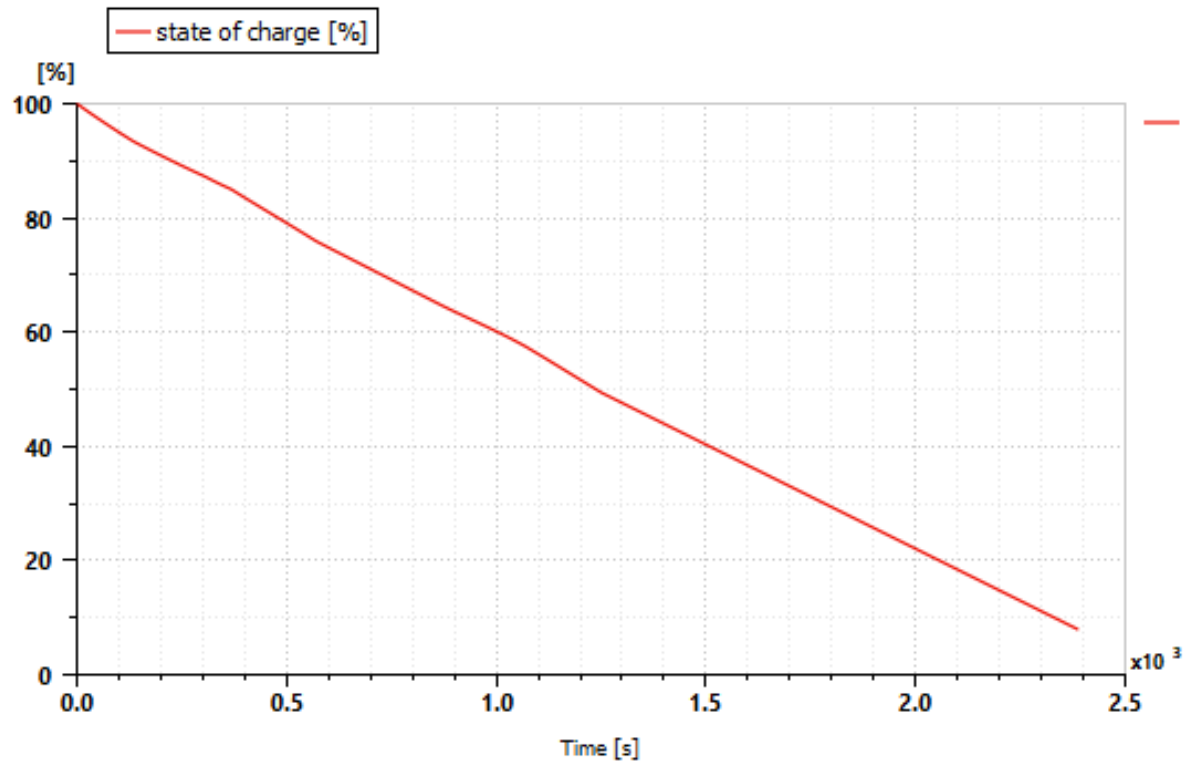


Figure 4.11 - *Battery's state of charge as mission develops*

In 4.11, we can see that the battery depletes until 78%.

Finally, lets look at the total consumption of fuel and the emissions produce as a byproduct of the combustion.

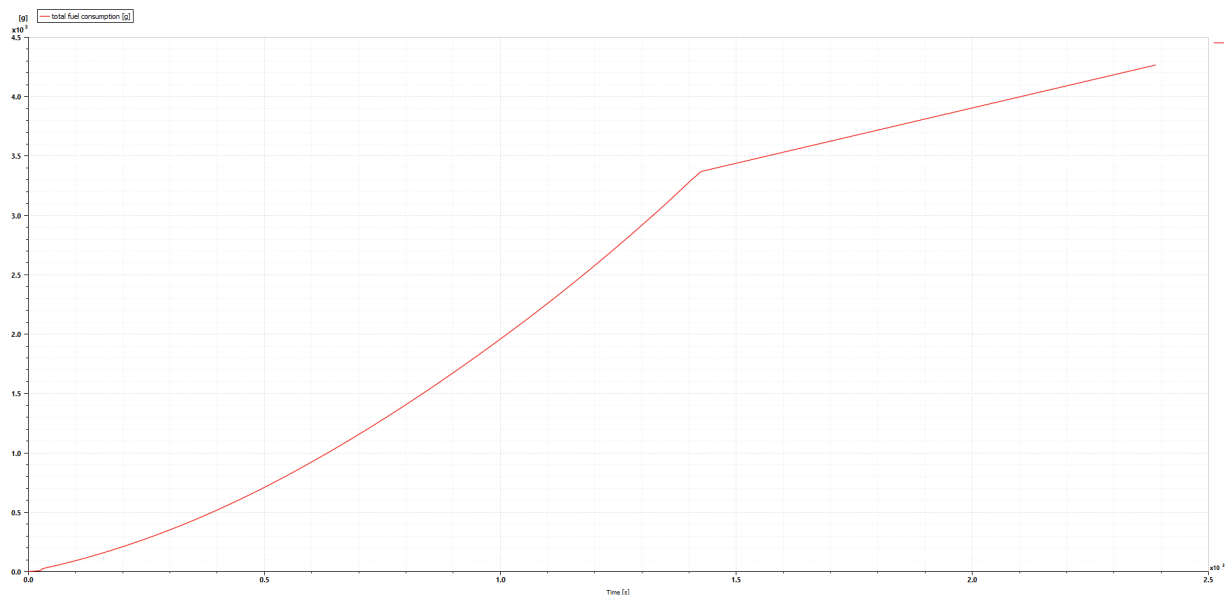


Figure 4.12 - *Amount of fuel consumption*

In this graph 4.12 we see that the total consumption of fuel reaches a total of 4.26 kg.

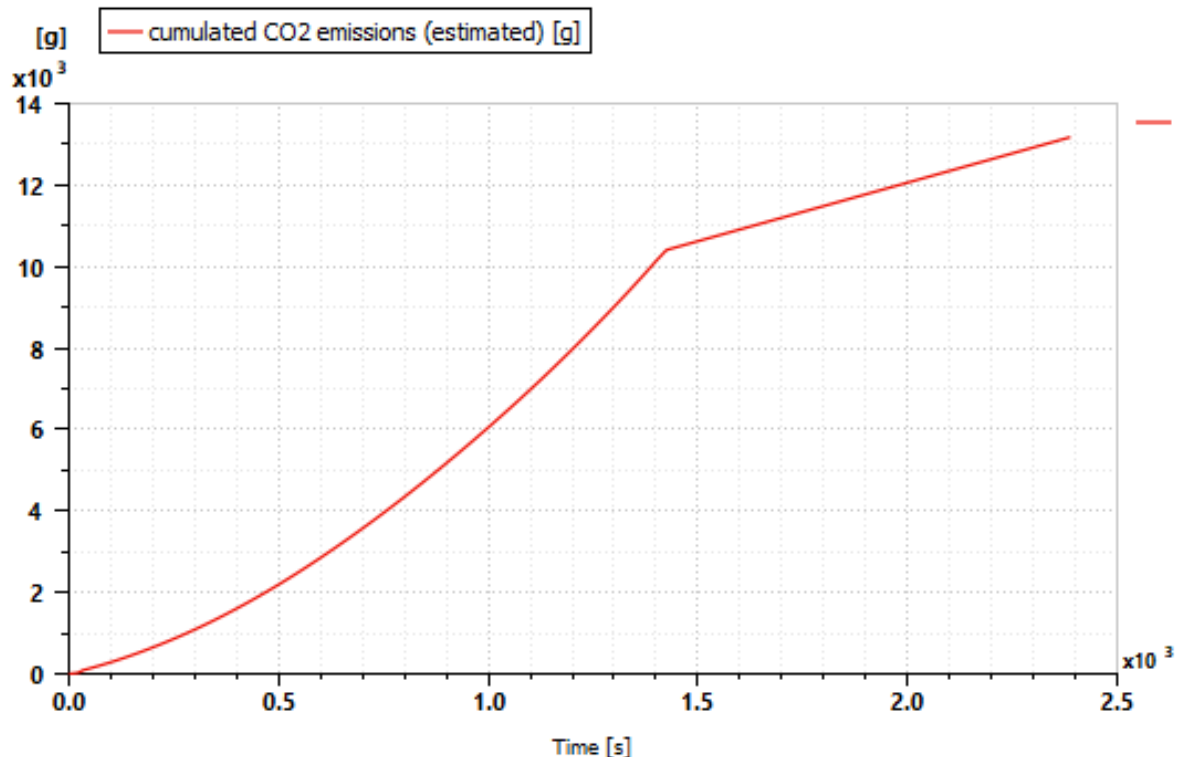


Figure 4.13 - *CO<sub>2</sub> produced*

Here, in 4.13, we are shown that the entire mission produces around 13 kg of CO<sub>2</sub>.

cumulated mass						
CO cumulated mass	3500.85 g	<input checked="" type="checkbox"/>	<input checked="" type="checkbox"/>	ref	2388.51	mCO
HC cumulated mass	305.652 g	<input checked="" type="checkbox"/>	<input checked="" type="checkbox"/>	ref	2388.51	mHC
NOx cumulated mass	21.4448 g	<input checked="" type="checkbox"/>	<input checked="" type="checkbox"/>	ref	2388.51	mNOx
soot cumulated mass	1.29499 g	<input checked="" type="checkbox"/>	<input checked="" type="checkbox"/>	ref	2388.51	msoot

Figure 4.14 - *Harmful pollutants produced*

Finally, these are the accumulated values for the emission of other pollutants which are commonly transferred to the atmosphere by the combustion of fossil fuels such as AVGAS.

## 4.2 Plots and graphs - TurboGenerator

In case of the usage of the TurboGenerator, this is the current produced by the generator encased in the supercomponent.

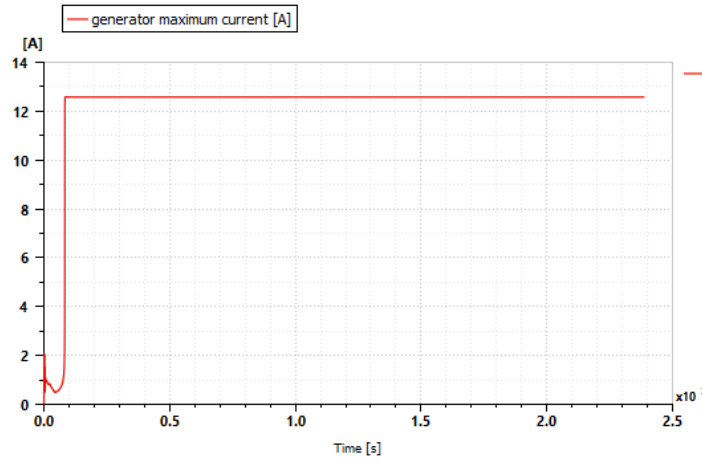


Figure 4.15 - *Current produced by the TurboGenerator*

Another important part of the simulation is the heat exchanger. This is the heat flow rate that it experiences.

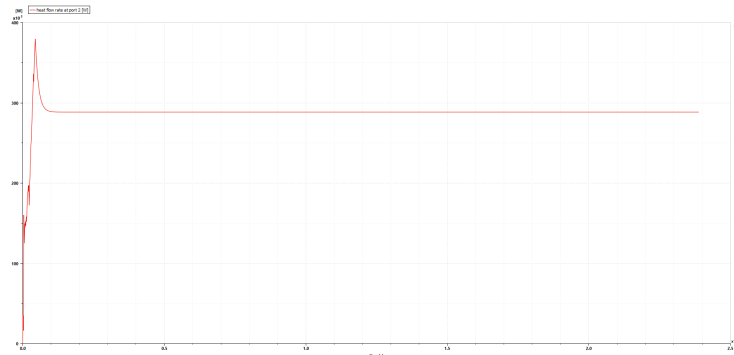


Figure 4.16 - *Heat flow going through the heat exchanger*

Finally, this is the torque that the turbine has been able to provide to the generator.

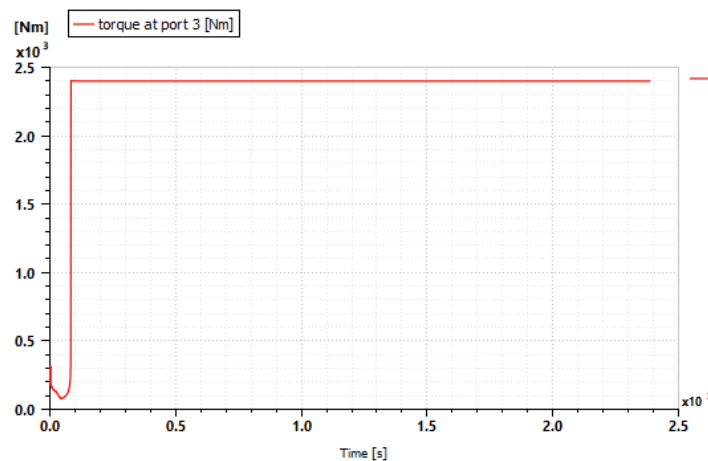


Figure 4.17 -

### 4.3 Interpretation of data and findings

The purpose of this study was to evaluate the impact of a series hybrid powertrain on an aircraft of small proportions. With the help of the simulation, we have been able to get enough numerical information to draw some conclusions of whether this types of designs can be used in a more frequent and common way. some of the key findings are:

1. The particular model of plane, the Mindus VP, is capable of safely completing the mission that was proposed since, it completed all the objectives for which it was designed and it safely made it back to the ground.
2. Keeping in mind that the purpose of the plane is to attract aircraft enthusiast and offer them a service, another quite important parameter would be to know the approximate operational cost of flying this type of airplane. In order to know this, we will take equations from [35].

$$Cost = x\beta W \rho_{bat} C_{batt} + (1 - x)\beta W \rho_{gas} C_{gas} \quad (4.1)$$

where:

- Cost: is the operational cost [€]
- x: percentage of hybrid
- $\beta$ : energy weight fraction
- W: weight of the plane [kg]
- $\rho_{bat}$ : energy density of the battery [kWh/kg]
- $C_{batt}$ : costs of battery's energy (electricity) [€/kWh]
- $\rho_{gas}$ : energy density of the gasoline [kWh/kg]
- $C_{gas}$ : costs of gasoline (AVGAS 100 LL) [€/kWh]

By following the next table 4.1, whose displayed data come from [23] for the price of non-household electricity and from [22] for the price of AVGAS 100 LL in Brussels International Airport.

Table 4.1 - *Prices for operational costs*

Product	Price in Belgium	Units
Non-household electricity	0.176	€/kWh
AVGAS 100 LL	0.2032	€/kWh

If we input the  $x_{max} = 97.12\%$ , which would accentuate the cost of the electricity, the operational costs would be  $C_{ost} = 24.93\text{€}$ . However, if we employ,  $x_{min} = 84.15\%$  then  $C_{ost} = 92.23\text{€}$ .

It is crucial to keep this figures in mind, even if this model is subjected to any changes, mainly due to the fact that in order to begin construction of this project and push it forward, it is necessary to go thoroughly over all the costs it implies. As engineers, expenses are something to always consider because, unfortunately, they heavily imply the feasibility of any idea and the amount of attention from investors and benefactors that it can attract

3. The biggest constraints that the current technology is facing, among many, are the efficiencies of internal combustion engines and the size of the batteries required. In this model, the  $\eta_{eng}$  only reached 32% at its peak while the battery came out at an outstanding weight of around 178 kg.

Regarding the engines, their inefficiency translates to higher fuel consumption and increased emissions, which are counterproductive to the environmental benefits sought by hybrid aviation. Additionally, ICEs operate optimally within a narrow range of conditions, many of which couldn't be considered during this study, making it difficult to achieve maximum efficiency across all phases of flight.

Considering batteries, they currently have a much lower energy density compared to aviation fuel, meaning that a large volume and mass are required to store the same amount of energy. This added weight and volume directly impacts the aircraft's performance, reducing its range and payload capacity.

Both areas require significant more investments and advancements to give a chance to hybrid aviation to prosper.

4. Common goals have to be reached to limit the emissions produced by aircraft's because, even though this model's emissions aren't as exaggerated as other aircraft, if many more companies start developing their own hybrid designs and selling them as if they had no impact on the environment, the purpose of the developing greener aviation will be neglected. As we have seen there are emissions in flights like these and they should be accounted for.
5. Results given by the simulation featuring the TurboGenerator aren't conclusive since the components are not modeled according to the true measures of the actual machine due to the lack of data. Even though the studied simulation follows the schematic of the machine, the RGT, choosing the right parameter with the amount of time available has been extremely difficult. Therefore some graphs show incorrect values such as states of charge higher than 100% or power generation way over the supposed maximum of 90 kW. Additional research on this machine and more studies about it are needed.

# Chapter 5

## Conclusion and future works

The end of this thesis is here at last and the final ideas shall be brought up at this point.

Hybrid aviation is the gateway to combine internal combustion engines with electric propulsion systems. This thesis has explored the possible benefits, challenges and solutions that these sorts of designs can feature. We have reviewed the goals that must be pursued in the future not only at the designer's level but also initiatives that have to be set at European levels.

This work has lead me to learn about aviation, one field that is extremely interesting both professionally and recreationally. Also, hybrid designs and technologies seem to be as a quite uncharted sector and that has been, for me personally, a great discovery that has taught me many valuable lessons. Another great thing about this project has been the usage of specialized software. This has been very enriching since, where I come from, practicing and designing with software such as this might be little underestimated and not enough attention is directed to these types of tools even though they are omnipresent in every industry nowadays.

In summary, hybrid aviation stands at the frontier of aerospace innovation, promising a greener and more efficient future for air travel. Continued research and development in ICE efficiency and battery technology are essential to overcoming current constraints, as it has been expressed in previous chapters. As advancements in these areas progress, hybrid aviation could become a viable and widespread solution, significantly contributing to the sustainability of the aviation industry.

# List of Figures

1.1	UN Initiatives for the future . . . . .	5
1.2	eFlyer 2 from Bye Aerospace . . . . .	6
1.3	E-Fan from Airbus . . . . .	7
1.4	E-Fan X from Airbus . . . . .	7
2.1	Lohner Porsche Mixte from 1901 . . . . .	9
2.2	Types of architectures for HEV . . . . .	11
2.3	Diagram of a Series Hybrid Electrical Coupling Drivetrain . . . . .	12
2.4	Diagram of a Parallel Hybrid Mechanical Coupling Drivetrain . . . . .	13
2.5	Original Series Hybrid Template . . . . .	14
2.6	Mission Profile Section . . . . .	15
2.7	Controls Section . . . . .	16
2.8	Cooling Section . . . . .	18
2.9	Electric Generation . . . . .	18
2.10	External controller . . . . .	19
2.11	Electrical motor . . . . .	20
2.12	Dual behavior of the model . . . . .	20
2.13	Main shaft . . . . .	21
2.14	Battery subsystem . . . . .	21
2.15	Propeller . . . . .	22
2.16	Aircraft . . . . .	24
2.17	Suspension's analogy . . . . .	25
2.18	Aerodynamic forces . . . . .	25
2.19	Engine by Rotax . . . . .	27
2.20	TurboGenerator by TurboTech . . . . .	28
2.21	Half cut of TurboGenerator . . . . .	28
2.22	Cirici by Airbus . . . . .	29
2.23	EcoPulse . . . . .	30
2.24	Mindus V1 by AOD . . . . .	31
2.25	Interior and ducted fan of Mindus V1 . . . . .	31
2.26	Extended landing gear of Mindus . . . . .	32
2.27	Upper view of Mindus . . . . .	34
2.28	Rotax 916 IS A . . . . .	35
2.29	Rotax 912 IS . . . . .	35
2.30	Rotax 915 IS A . . . . .	36
2.31	Rotax 912 ULS . . . . .	36
2.32	Rotax 914 UL . . . . .	36
2.33	Rotax 912 UL . . . . .	37
2.34	Rotax 912 UL . . . . .	37
2.35	Virus SW 80 by Pipistrel . . . . .	37
2.36	Performance of the Rotax 912 UL . . . . .	38

2.37 Consumption of the Rotax 912 UL . . . . .	39
2.38 Safran's Logo . . . . .	40
2.39 Safran's products . . . . .	41
2.40 GENeUS 300 electric generator . . . . .	42
2.41 Cassio 330 . . . . .	43
2.42 ENGINEUS 45 for Cassio 330 . . . . .	43
2.43 GENeUSPACK . . . . .	44
2.44 Propeller of the ducted fan . . . . .	45
2.45 Profile of the blade . . . . .	46
2.46 Maps of $C_t$ and $C_p$ for our rotor . . . . .	46
2.47 Efficiency map . . . . .	46
2.48 TurboGenerator Simulation . . . . .	47
2.49 Air Composition . . . . .	48
2.50 Compressor Map . . . . .	49
2.51 Turbine map . . . . .	49
3.1 Flight Plan . . . . .	50
3.2 Atmospheric Parameters . . . . .	52
3.3 Power required without the correcting factor . . . . .	53
3.4 Fully working model of a Diesel Combustion Engine . . . . .	54
3.5 Power demand signal and the according flight phases . . . . .	54
3.6 Performance of the engine . . . . .	55
3.7 Calculated values for the grams of pollutants per hour . . . . .	56
3.8 Multiple 1D table of fuel consumption . . . . .	60
3.9 Weight loss by consumption . . . . .	61
3.10 Coefficient of lift as a function of angle of attack . . . . .	61
3.11 Final equations for $C_d$ . . . . .	62
4.1 Flight Mission vs Actual Flight . . . . .	64
4.2 Coefficients . . . . .	64
4.3 Lift-to-drag ratio . . . . .	65
4.4 Lift vs Drag . . . . .	65
4.5 Propulsive power coming from the fan in reaction with each flight phase . . . . .	66
4.6 Torque signal provided by the electric motor . . . . .	66
4.7 Torque signal provided by Rotax 912 UL . . . . .	67
4.8 Torque signal provided by Rotax 912 UL . . . . .	67
4.9 Engine efficiency of the Rotax 912 UL . . . . .	68
4.10 Electrical power from the GENeUS 300 . . . . .	68
4.11 Battery's state of charge as mission develops . . . . .	69
4.12 Amount of fuel consumption . . . . .	69
4.13 CO <sub>2</sub> produced . . . . .	70
4.14 Harmful pollutants produced . . . . .	70
4.15 Current produced by the TurboGenerator . . . . .	71
4.16 Heat flow going through the heat exchanger . . . . .	71
4.17 . . . . .	71

# List of Tables

2.1	New limits for the 6 classes of ULM . . . . .	32
2.2	Rotax 912 ULS Performance Specifications . . . . .	39
3.1	Constraints of the hybrid design . . . . .	59
4.1	Prices for operational costs . . . . .	72

# Bibliography

- [1] Aerospace Technologie. E-Fan Electric Aircraft. Accessed: 14/05/2024.
- [2] European Union Aviation Safety Agency. Easa pro, 2002. Accessed: 20/5/2024.
- [3] Ailes Anciennes Toulouse. AIRBUS E-FAN, 2020. Accessed: 14/05/2024.
- [4] Airbus. E-Fan Electric Aircraft. Accessed: 14/05/2024.
- [5] Airbus. EcoPulse demonstrator takes first flight with batteries onboard. Accessed: 14/05/2024.
- [6] Airbus. The EcoPulse aircraft demonstrator makes first hybrid-electric flight. Accessed: 14/05/2024.
- [7] Robert W. Bulaga Chief Engineer Anita I. Abrego Aerospace Engineer. Performance study of a ducted fan system. Technical report, NASA Ames Research Center, 2002.
- [8] Bye Aerospace. eFlyer, 2021. Accessed: 14/05/2024.
- [9] Mustafa Cavcar. The international standard atmosphere (isa). Academic report, Anadolu University.
- [10] Defense Technical Information Center. *Handbook of Aviation Fuel Properties*. COORDINATING RESEARCH COUNCIL INCORPORATED, 1983.
- [11] FAUVET Damien. Turbomachine, notamment turbogénérateur et échangeur pour une telle turbomachine., November 2016.
- [12] Ministère de la transition écologique et de la cohésion de territoires. Arrêté du 23 septembre 1998 relatif aux aéronefs ultralégers motorisés, 1998. Accessed: 20/5/2024.
- [13] Francesco De Marco. Comparative study of multiphysics modelling and simulation software for lifetime performance evaluation of battery systems. Master's thesis, Aalto University, School of Engineering, Politecnico di Torino, 2023.
- [14] Mehrdad Ehsani. *Modern Electric, Hybrid Electric and Fuel Cell Vehicles*. Taylor Francis, CRC Press ©2019, third edition, 2018.
- [15] Safran Electric and Power. Safran and cuberg announce collaboration agreement on battery systems for advanced electric aviation. Accessed: 9/6/2024.
- [16] Safran Electrical and Power. Batteries: Safran at the forefront of electric propulsion. Accessed: 3/6/2024.
- [17] Safran Electrical and Power. Engineus™ smart electric motors. Accessed: 2/6/2024.

- [18] Safran Electrical and Power. Geneus™ smart generator. Accessed: 2/6/2024.
- [19] Rotax Aircraft Engines. Aircraft engines. Accessed: 26/5/2024.
- [20] Rotax Aircraft Engines. As time flies by, 2020. Accessed: 25/5/2024.
- [21] Rotax Aircraft Engines. Operators manual: Rotax 912 ul, 2024. Accessed: 26/5/2024.
- [22] AOPA Europe. Fuelprice overview. Accessed: 10/6/2024.
- [23] Eurostat Stadistics Explained. Electricity price statistics. Accessed: 10/6/2024.
- [24] FFPLUM. Ulm : Nouvelle reglementation 2019. PDF, 2019.
- [25] Snorri Gudmundsson. *General Aviation Aircraft Design: Applied Methods And Procedures*. Butterworth-Heinemann, Elsevier Inc, ©2014, first edition, 2014.
- [26] Pilot Magazine. Turbotech's mission: make the small aircraft turboprop a reality. *Pilot*, November 2022.
- [27] Engineering National Academies of Sciences and Medicine. *Exhaust Emissions from In-Use General Aviation Aircraft*. The National Academies Press, Washington, DC, 2016.
- [28] Graham Warwick Aviation Week Network. Safran aims to be first to certify electric engine. Accessed: 2/6/2024.
- [29] OAD. Mindus-dp. PDF, 2020. Etude conceptuelle.
- [30] Department of Economic and Social Affairs of the United Nations. The 17 goals, 2015.
- [31] Safran. History and hertitage, 2018. Accessed: 30/5/2024.
- [32] Market Screener. Safran electrical power successfully completes first geneus 300 ground test campaign. Accessed: 2/6/2024.
- [33] Siemens Amesim software. *Simcenter Amesim Demos*. Siemens, Simcenter Amesim, v2304 edition, 2023.
- [34] TurboTech. The ultimate hybrid-electric solution - turbogenerator, 2022.
- [35] Tsz Him Yeung. Optimal battery weight fraction for serial hybrid propulsion system in aircraft design. Master's thesis, Embry-Riddle Aeronautical University, Daytona Beach, Florida, USA, 2019. Dissertations and Theses. 457.